

UNIVERSIDADE DE SÃO PAULO

Instituto de Ciências Matemáticas e de Computação

**The graph representation problem for the investigation of
synchronies in networks**

Tiago de Albuquerque Amorim

Tese de Doutorado do Programa de Pós-Graduação em
Matemática (PPG-Mat)

SERVIÇO DE PÓS-GRADUAÇÃO DO ICMC-USP

Data de Depósito:

Assinatura: _____

Tiago de Albuquerque Amorim

The graph representation problem for the investigation of synchronies in networks

Doctoral dissertation submitted to the Instituto de Ciências Matemáticas e de Computação – ICMC-USP, in partial fulfillment of the requirements for the degree of the Doctorate Program in Mathematics.
FINAL VERSION

Concentration Area: Mathematics

Advisor: Profa. Dra. Miriam Garcia Manoel

USP – São Carlos
May 2024

Ficha catalográfica elaborada pela Biblioteca Prof. Achille Bassi
e Seção Técnica de Informática, ICMC/USP,
com os dados inseridos pelo(a) autor(a)

A524t Amorim, Tiago de Albuquerque
The graph representation problem for the
investigation of synchronies in networks / Tiago de
Albuquerque Amorim; orientadora Miriam Garcia
Manoel. -- São Carlos, 2024.
85 p.

Tese (Doutorado - Programa de Pós-Graduação em
Matemática) -- Instituto de Ciências Matemáticas e
de Computação, Universidade de São Paulo, 2024.

1. network. 2. synchrony. 3. symmetry. 4.
Laplacian matrix. I. Manoel, Miriam Garcia, orient.
II. Título.

Tiago de Albuquerque Amorim

O problema da construção de grafos para o estudo de
sincronias em redes

Tese apresentada ao Instituto de Ciências
Matemáticas e de Computação – ICMC-USP,
como parte dos requisitos para obtenção do título
de Doutor em Ciências – Matemática. *VERSÃO
REVISADA*

Área de Concentração: Matemática

Orientadora: Profa. Dra. Miriam Garcia Manoel

USP – São Carlos
Maio de 2024

*Este trabalho é dedicado à minha mãe, Marina Judite,
e à minha avó, Marina Bezerra.*

ACKNOWLEDGEMENTS

Este é o momento difícil da tese em que queremos agradecer a todos que passaram pelas nossas vidas e que deixaram um sorriso, um ensinamento, um desafio, uma saudade, uma motivação, que nos servem de exemplos em questões pontuais ou que são exemplos para toda a vida. Eu precisaria de um texto do tamanho desta tese para conseguir agradecer a todos, sem esquecer ninguém. Então, aqui irei falar de pessoas que, sem sombra de dúvidas, mudaram a forma como vejo o mundo e me deixaram cada vez mais próximo do meu doutorado.

Quero agradecer primeiramente aos meus pais: José Carlos, meu pai, que me mostrou que a melhor forma de alcançar nosso objetivo é com trabalho bem feito e constante; Marina Judite, minha mãe, que me mostrou que a melhor forma de viver é sempre com amor, carinho e respeito a todos. Observando como eles levam suas vidas, aprendi que os momentos de maior aprendizado são quando ajudamos e servimos quem está próximo a nós, e foi isso o que tentei fazer ao longo desses 12 anos de graduação, mestrado e doutorado. Nunca foi sobre competição, sempre foi sobre cooperação.

Muito obrigado à minha professora da 2ª série do fundamental, tia Jane, que já me dizia que eu seria um matemático, e cá estou defendendo a minha tese. Muito obrigado ao professor Edson, que no meu 1º ano do ensino médio me mostrou a noção de limite, me motivou com matemática avançada, e isso facilitou muito a graduação.

Quero agradecer aos professores Sérgio Santa Cruz, Antônio Carlos, Hildeberto Eulálio e Henrique Vitória, meus professores da graduação e mestrado. Eu sempre amei matemática, mas eles me ensinaram a estudar matemática.

Muito obrigado mesmo à minha orientadora, Professora Miriam Garcia Manoel, pela escolha do tema de pesquisa, pelas conversas sempre produtivas, pelas perguntas-chave que me fizeram avançar na pesquisa, pela paciência com meus erros recorrentes de português e inglês, por estar sempre com um sorriso no rosto e sempre se preocupar com o meu bem-estar.

Muito obrigado aos professores Fernando Martins Antoneli Jr e Ronaldo Alves Garcia pelas conversas certas que acenderam uma luz indicando um caminho quando eu estava perdido na pesquisa.

Aos amigos que fiz aqui na USP: Amanda, Andrés, Castelo, Eliada, Gabriel, Igor, Ivan, Juniomar, Maíra, Raphael, Reji, Verônica... (são muitos mesmo e ainda tem muitos mais). Se eu ganhasse na loteria, daria um milhão de reais para cada um de vocês, mas infelizmente ainda não ganhei. Então, dedico a cada um de vocês um milhão de abraços por me acolherem

de imediato e tornarem esses últimos 4 anos (com uma pandemia no meio) especiais. Para Ana Paula, um amor que conheci aqui em São Carlos, daria metade do restante do prêmio. Muito obrigado a todos vocês!!

Um profundo e sincero agradecimento a todos no ICMC, funcionários e professores. Em especial ao grupo de Singularidades.

Por fim, agradeço ao CNPq pelo apoio financeiro no período de mar/2019 a jul/2019 e agradeço à FAPESP pelo apoio financeiro no período de ago/2019 a fev/2024 (número do processo 2019/21230-0).

RESUMO

AMORIM, T. **O problema da construção de grafos para o estudo de sincronias em redes.** 2024. 85 p. Tese (Doutorado em Ciências – Matemática) – Instituto de Ciências Matemáticas e de Computação, Universidade de São Paulo, São Carlos – SP, 2024.

Uma rede de células é um grafo dotado de uma relação de equivalência que preserva o conjunto de entrada dos vértices que permite uma caracterização dos campos vetoriais admissíveis que regem a dinâmica da rede de acordo com os tipos de acoplamento desse grafo. Neste contexto, esta tese tem dois objetivos. O primeiro vai no sentido de responder ao problema inverso: para $n \geq 2$, qualquer mapa em \mathbb{R}^n pode ser realizado como um campo vetorial admissível para algum grafo com o número de vértices dependendo de (mas não necessariamente igual a) n . Dado um mapa, apresentamos um procedimento para construir todos os grafos admissíveis não equivalentes, para uma relação de equivalência apropriada. Também fornecemos um limite superior para o número de tais grafos. Como consequência, subespaços invariantes sob o campo vetorial podem ser investigados como o lugar geométrico dos estados de sincronia de um grafo admissível, no sentido de que um grafo adequado pode ser escolhido para realizar acoplamentos com mais (ou menos) sincronia do que outro grafo admissível para o mesmo campo vetorial. A abordagem fornece, em particular, uma investigação sistemática da ocorrência de *estados de quimera* em uma rede de osciladores idênticos de van der Pol. Como segundo objetivo, a partir do impacto dos resultados de sincronização das redes de Kuramoto, introduzimos a classe generalizada de redes Laplacianas, governadas por mapas cujo Jacobiano em qualquer ponto é uma matriz simétrica no qual cada linha tem soma nula de suas entradas. Ao reconhecer esta matriz como um Laplaciano com pesos do grafo associado, deduzimos estimativas ótimas de seus autovalores positivos, nulos e negativos diretamente da topologia do grafo. Além disso, fornecemos uma caracterização dos mapas que definem as redes Laplacianas. Por último, discutimos a estabilidade do equilíbrio dentro de subespaços de sincronia para dois tipos de redes Laplacianas em um anel com alguns acoplamentos extras.

Palavras-chave: rede, grafo, campo vetorial admissível, sincronia, simetria, matrix Laplaciana, singularidade.

ABSTRACT

AMORIM, T. **The graph representation problem for the investigation of synchronies in networks.** 2024. 85 p. Tese (Doutorado em Ciências – Matemática) – Instituto de Ciências Matemáticas e de Computação, Universidade de São Paulo, São Carlos – SP, 2024.

A coupled cells network is a graph endowed with an input-equivalence relation on the set of vertices that enables a characterization of the admissible vector fields that rules the network dynamics according to the coupling types of that graph. In this context, this thesis has two targets. The first one goes in the direction of answering an inverse problem: for $n \geq 2$, any mapping on \mathbb{R}^n can be realized as an admissible vector field for some graph with the number of vertices depending on (but not necessarily equal to) n . Given a mapping, we present a procedure to construct all non-equivalent admissible graphs, up to an appropriate equivalence relation. We also give an upper bound for the number of such graphs. As a consequence, invariant subspaces under the vector field can be investigated as the locus of synchrony states supported by an admissible graph, in the sense that a suitable graph can be chosen to realize couplings with more (or less) synchrony than another graph admissible to the same vector field. The approach provides in particular a systematic investigation of occurrence of *chimera states* in a network of van der Pol identical oscillators. As a second target, from the impact of the results about synchronization in Kuramoto networks, we introduce the generalized class of Laplacian networks, governed by mappings whose Jacobian at any point is a symmetric matrix with row entries summing to zero. By recognizing this matrix as a weighted Laplacian of the associated graph, we derive the optimal estimates of its positive, null and negative eigenvalues directly from the graph topology. Furthermore, we provide a characterization of the mappings that define Laplacian networks. Lastly, we discuss stability of equilibria inside synchrony subspaces for two types of Laplacian networks on a ring with some extra couplings.

Keywords: network, graph, admissible vector field, synchrony, symmetry, Laplacian matrix, singularity.

LIST OF FIGURES

Figure 1 – An admissible nonregular simple graph (on the left) and an admissible regular multigraph (on the right) for the system of equations (1.1).	21
Figure 2 – (a) A 3-cell graph with distinct couplings and (b) a 3-cell graph with identical couplings.	38
Figure 3 – Admissible graph \mathcal{G}_2 for (4.10) with six \sim_2 -classes.	41
Figure 4 – Admissible graph \mathcal{G}_3 for (4.10) with three \sim_3 -classes.	41
Figure 5 – Admissible graphs \mathcal{G}_4^1 (left) and \mathcal{G}_4^2 (right) for (4.10) with two \sim_4 -classes.	42
Figure 6 – An admissible graph \mathcal{G}_2 for (4.10) seen as a network of 3 cells.	42
Figure 7 – An admissible graph \mathcal{G}_4 for (4.10) seen as a network of 2 cells.	42
Figure 8 – An admissible graph \mathcal{G}_4 for (4.10) seen as a network of 2 cells.	43
Figure 9 – A nonhomogeneous bidirected graph with six identical cells and two types of edges.	60
Figure 10 – G_6	62
Figure 11 – The disconnected graph obtained from G_6 by assigning $Jf(x)$ as the weighted Laplacian, for $x = (0, 0, \pi/2, \pi, \pi, 3\pi/2)$	65
Figure 12 – A homogeneous \tilde{G}_6	66

LIST OF TABLES

Table 1	– Synchrony patterns of the network graph G_6 together with their symmetries.	53
Table 2	– Admissible network graphs for (4.18) up to ODE-equivalence with their corresponding synchrony patterns. The last column gives the number of admissible graphs nonisomorphic and ODE-equivalent to the graph.	54
Table 3	– The first column indicate the synchrony patterns extracted from Table 1; the corresponding class of critical points is given in the second column by a representative up to the symmetries of $Aut(G_6)$; the last column gives the number n_+ of positive eigenvalues of the Jacobian at the corresponding critical point; the remaining three columns are the data used to apply Theorem 5.1. . .	68

CONTENTS

1	INTRODUCTION	19
2	COUPLED CELL NETWORKS	27
2.1	Coupled Cell Networks	27
2.2	Admissible vector fields	28
2.3	ODE-equivalence	30
3	SYNCHRONY AND SYMMETRY	31
3.1	Synchronies from invariant subspaces	32
3.2	Synchrony and symmetry in regular networks	33
4	THE REALIZATION OF ADMISSIBLE GRAPHS FOR COUPLED VECTOR FIELDS	37
4.1	The stepwise procedure	38
4.2	Example: a vector field on \mathbb{R}^4	41
4.3	Simple graph versus multigraph	43
4.4	Relation among admissible graphs	43
4.5	Example: a vector field on \mathbb{R}^6	48
4.6	Coupled network of van der Pol identical oscillators	50
5	SYNCHRONY PATTERNS IN LAPLACIAN NETWORKS	55
5.1	Graph Laplacian matrix	55
5.2	Laplacian mappings	56
5.3	Laplacian networks with additive structure	59
5.4	Critical points on synchrony subspaces of additive Laplacian networks	61
5.4.1	<i>Total synchrony subspace</i>	61
5.4.2	<i>Kuramoto network with G_6 coupling</i>	62
5.4.3	<i>A homogeneous network \tilde{G}_6 with two types of couplings</i>	65
6	FUTURE RESEARCH	69
	BIBLIOGRAPHY	71
APPENDIX A	ALGORITHM TO LIST SYNCHRONY SUBSPACES FOR BIDIRECTED REGULAR NETWORKS	75

INTRODUCTION

Dynamical systems with special structures are very common in applications. The special structure arises due to some characteristic of the phenomenon one is trying to model. Among the most important classes of dynamical systems with special structures are the Hamiltonian systems, where there is conservation of energy; the conservative systems, where there is preservation of a smooth measure; the reversible systems, where there is invariance under time-reversion and the equivariant systems, where there is invariance under a group of spatial symmetries. In each of these classes there are a number of typical or generic behaviors which from the point of view of general dynamical systems (i.e. without any special structure) are extremely non-generic. Coupled cell networks are another class of dynamical systems with special structure that have been motivated by applications in neuroscience and biology, for example. We go back to the 80's to recall physical, biological, mechanical systems that have been interpreted in many ways as coupled systems; for example, Josephson junction arrays ([HADLEY; BEASLEY; WIESEN-FELD, 1988](#)), semiconductor coupled lasers or multimode solid state laser systems in ([WANG; WINFUL, 1988](#)) and ([BRACIKOWSKI; ROY, 1991](#)), central pattern generators and symmetric chains of weakly coupled oscillators in ([KOPELL; ERMENTROUT, 1986](#)), ([KOPELL; ERMENTROUT, 1988](#)) and ([KOPELL; ERMENTROUT, 1990](#)), sympatric speciation ([STEWART; ELMHIRST; COHEN, 2003](#)), normal mode vibrations of a loaded string and linear motion of a triatomic molecule ([FOWLES; CASSIDAY *et al.*, 1986](#)), the classical n -body dynamics ([STEPHAN, 1987](#)), among many others. It was around 2002 that the authors M. Golubitsky, I. Stewart and collaborators (([GOLUBITSKY; NICOL; STEWART, 2004](#)), ([GOLUBITSKY; STEWART, 2003](#)), ([GOLUBITSKY; STEWART; TÖRÖK, 2005](#)), ([STEWART; GOLUBITSKY; PIVATO, 2003](#))) started to formulate the notion of a *coupled cell network*, a rich systematic way to study coupled dynamics under a graph theory formalism ([GOLUBITSKY; STEWART, 2003](#)), establishing a general setting for simple graphs (no multiarrows or loops) ([STEWART; GOLUBITSKY; PIVATO, 2003](#)) and for multigraphs (possible multiple arrows and loops) ([GOLUBITSKY; STEWART; TÖRÖK, 2005](#)). Under that formulation, a network graph is more than

a finite set of vertices with a finite set of arrows, for there are distinct types of vertices and arrows to be taken into consideration to represent abstractly a system of ordinary differential equations (ODEs) equipped with interacting individual cells as canonical observables. Each vertex represents an individual cell which is governed by an autonomous system of ODEs, and the set of edges encodes couplings, so that a well defined ‘admissible’ vector field is assigned to this network graph. One of the main features of these approaches is the possibility to formulate and prove generic properties in the context of coupled cell networks.

A central matter is to know to what extent the rigidity of the network graph topology constrains the investigation of the associated dynamics. It is well known that topologically distinct network graphs can lead to the same set of admissible vector fields (see (GOLUBITSKY; STEWART; TÖRÖK, 2005)). Hence, as naturally expected, this formalism is largely based on different kinds of equivalence relations, as we briefly mention in what follows. One key identification of the cells inside a network is the notion of ‘input isomorphism’ (STEWART; GOLUBITSKY; PIVATO, 2003), under which two cells are equivalent if the dynamics of the cells are governed by the same differential equations, up to a permutation of the variables. Another identification is defined by the ‘balanced equivalence relation’ between cells, which stratifies the set of cells in terms of equalities among cell variables representing a synchrony state of the network. This is a major topic in the investigation of coupled dynamics, with a countless number of works devoted to it. The authors in (AGUIAR; DIAS, 2014) present an algorithm that generates the lattice of synchrony subspaces of a given network graph. We have implemented this algorithm for Wolfram Mathematica language in Appendix A. Balanced equivalence relations are also a strong reason for the setting of the multigraph formalism, that is, for graphs with multiple arrows of same type connecting two vertices, since the associated quotient graphs – those that encode the synchronies in the network – are generally multigraphs. Alongside these relations, much attention has also been driven to relations between networks, namely the ‘automorphisms’ of a network graph (formalized in (ANTONELI; STEWART, 2006)) and the ‘ODE-equivalence’ between networks (see (DIAS; STEWART, 2005) and (STEWART; GOLUBITSKY; PIVATO, 2003) for example). Two nonisomorphic networks can have equivalent dynamical behavior, and this is detected by ODE-equivalence.

The realization of admissible graphs for coupled vector fields

If we look at the usual way of modelling a coupled dynamics through an associated vector field, relevant distinctions emerge in assigning a simple graph (one edge of a type connecting two vertices), or a multigraph, that realizes it as its admissible vector field. It is expected that this assignment is not unique – just take two distinct network graphs inside an ODE-equivalence class, possibly one chosen to be a simple graph and the other to be a multigraph. However, a more subtle case is equally possible, as it is shown with the elementary example below, also illustrating that, although it may be simpler to deal with simple graphs, multiple arrows are sometimes the appropriate way to model certain couplings. Consider the following differential

equations on \mathbb{R}^3 ,

$$\begin{aligned}\dot{x}_1 &= x_1 + x_1^3 \\ \dot{x}_2 &= x_2 + x_2^2 x_3 \\ \dot{x}_3 &= x_3 + x_1 x_2 x_3.\end{aligned}\tag{1.1}$$

These equations can model a 3-cell network represented by the simple directed graph of Fig. 1 (left), which is an inhomogeneous graph with cells with distinct valencies. However, the same equations can also model a network represented by the multigraph of Fig. 1 (right), which is a regular graph, with all cells of same type and same input and all arrows of same type, which therefore presents synchronies. In Section 4.3 we return to this example. Now, if, on one hand, from a given graph and a predetermined set of cell domain there is a unique general form of an admissible vector field, the inverse problem, on the other hand, is not uniquely solved, as the example above shows. For this elementary example, the possible synchronous configurations for both graphs coincide, namely total synchrony and total asynchrony, but this is not the case in general, as we shall see in many examples here.

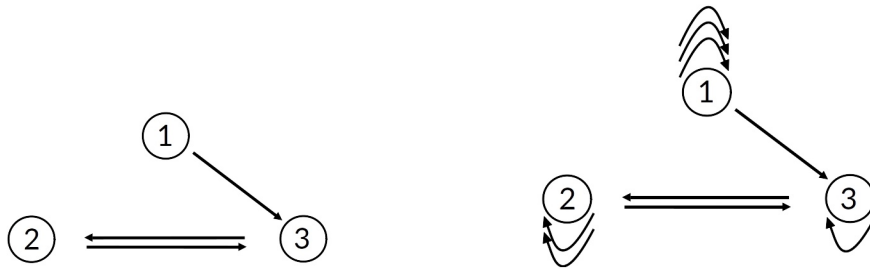


Figure 1 – An admissible nonregular simple graph (on the left) and an admissible regular multigraph (on the right) for the system of equations (1.1).

In distinct areas of applied science, the possible distinct couplings that can be arranged from a given vector field modeling an interacting dynamical system is a relevant problem to be understood. The aim here is to discuss and solve this inverse problem in general. For a given vector field, we construct non ODE-equivalent graphs that realize it as their admissible vector field, which we shall call ‘admissible graphs’. This stepwise procedure is presented in the Section 4.1. This is an interesting question even when the vector field is already defined in terms of some network structure.

In order for a vector field to be a candidate to model a coupled dynamics with nontrivial coupling, the starting point is to choose the number of cells as well as the dimensions of the cell variables. Next, we look at symmetries, namely invariance of its component functions under permutations of (sets of) variables; for example, if the components of the vector field are invariant under all the permutations of its variables, then there is only one resulting admissible graph, which is a homogeneous graph. Symmetries are then related to the assignment of *generating functions* to the components of the vector field and, as we shall see, this is closely related to the number of distinct admissible graphs. We remark that there are special cases for which two

distinct such choices may lead to network graphs whose synchronies can be related, in the sense that one is deduced from the other (see Section 4.6).

As already mentioned above, isomorphic graphs and more generally ODE-equivalent graphs must be identified in the search of distinct types of dynamics. Our procedure takes these identifications into consideration, producing the complete list of non ODE-equivalent graphs that can be realized from a given vector field. As our first main results we also give in Proposition 4.2 an upper bound for the number of elements in this list and we establish relationships between all admissible graphs in the Theorems 4.3 and 4.7.

One particular motivation to carry out with this procedure relies on several approaches to study ‘chimera’ states of a vector field (Section 4.6). We cite (ABRAMS; STROGATZ, 2006), (KURAMOTO; BATTOGTOKH, 2002), (PANAGGIO; ABRAMS, 2015), (MARTENS *et al.*, 2013), (SIMO *et al.*, 2021) for example, and (ZAKHAROVA, 2020) for a timely overview on the subject. A chimera state is a peculiar partial synchronization pattern in networks, defined as a spatio-temporal pattern in which a system of identical oscillators is split into coexisting regions of coherent (phase and frequency locked) and incoherent (drifting) oscillation (ABRAMS; STROGATZ, 2006). Hence, it is a state in which the whole set of cells is broken into a synchronous part and an asynchronous part. This is a phenomenon in interacting populations of intense research efforts in physical, biological, chemical and social systems (ACEBRÓN *et al.*, 2005). We notice that although a well-known phenomenon in non-identical coupled oscillators, the coexistence of coherence and incoherence was observed by Kuramoto and Battogtokh for a system of identical oscillators (KURAMOTO; BATTOGTOKH, 2002); we refer to (PANAGGIO; ABRAMS, 2015) for a comprehensive list of references about this subject. In these works, the research is carried out from a model given by a vector field, based on numerical or analytical investigation of the set of the proposed equations. For example, the authors in (MARTENS *et al.*, 2013) carry out numerical simulations of a mechanical experiment with two subpopulations of identical metronomes on two coupled swings with chimera states emerging robustly. In this experiment, we observe that the modeling equations admit an invariance under the permutation of the two subsets of metronomes that has not been taken into account apparently, and this might reveal distinct chimera states. Our procedure is in particular a way to describe chimeras from the possible synchronized states that appear from the graphs admissible from the given vector field. In this setting, the analysis of robust attracting chimeras should correspond to the numerically observed chimeras, and this is one of our interests for near future work. Section 4.6 is addressed to expand on this topic in more detail with a concrete example.

Synchrony patterns in Laplacian networks

About fifty years ago Kuramoto introduced in (KURAMOTO, 1975) a system of ordinary differential equations that has since gained recognition as the simple (or traditional) Kuramoto model. It has been proposed as a straightforward and solvable framework to comprehend mutual synchronization within a cluster of oscillators that are equally coupled to all other oscillators. Its

significance is further underscored by its applications across various synchronization scenarios in chemical (CZAJKOWSKI; BATISTA; VIANA, 2023), biological (VANDERMEER *et al.*, 2021), social systems and in neuroscience phenomena (NOVIKOV; BENDERSKAYA, 2014). Since then, numerous related articles have emerged in the literature in distinct contexts of investigation, varying from numerical analysis and stochastic methods (KOTWAL; JIANG; ABRAMS, 2017) to criteria for the existence and stability of (clusters of) synchrony (BRONSKI; CARTY; DEVILLE, 2021). In this thesis we introduce a more comprehensive framework for this particular type of system of coupled identical individual systems, accounting for two distinct aspects:

- the coupling may not necessarily be universally applied across all elements;
- the Jacobian of the network vector field is a general Laplacian matrix.

As we shall see, the second requires that being bidirected is a necessary condition for the associated graphs. We remark that the second aspect appears naturally in gradient systems of coupled cell networks with an extra \mathbf{S}^1 -invariance condition on the vector field components; see (MANOEL; ROBERTS, 2015), where critical points are investigated for cells coupled in a ring. In fact, as our second main result we prove that vector fields with a Laplacian structure are gradient; see Theorem 5.9.

Recall from algebraic graph theory that eigenvalues of a weighted graph Laplacian matrix hold substantial information of the graph. For instance, it follows directly from the definition that zero is an eigenvalue, associated with the eigenvector $(1, \dots, 1)$. This condition is already interesting from the point of view of the local dynamics, as it implies that there are no isolated singularities. Furthermore, in the case of non-negative weights, it is well known that all the eigenvalues are non-negative and the algebraic multiplicity of the zero eigenvalue is exactly the number of connected components of the graph. This result has been extended in (BRONSKI; DEVILLE, 2014) to the case of connected graphs allowing negative weights. Since it is expected that the Jacobian matrix of the vector field has zero entries, recognizing this matrix as the graph Laplacian naturally leads us to the inherent condition that the graph may be disconnected. With the requirement to address this condition, we have interpreted the absence of an edge connecting two vertices as the existence of an edge with zero weight to extend the result to disconnected graphs; see Theorem 5.1. The result is the optimal estimate for the number of negative, null and positive eigenvalues from the number of connected components of the subgraph determined by positive weights and the subgraph determined by negative weights.

In the study of local dynamics, specially in bifurcation theory, the starting point is the analysis of existence and nature of equilibria and periodic orbits. An equilibrium is a critical point of the vector field expected to lie on subspaces that are invariant under the dynamics. In equivariant dynamics, these are fixed-point subspaces of subgroups of the symmetry group; in coupled networks, these are synchrony subspaces determined from the associated graph.

We now raise the issue regarding a connection between synchrony and symmetries of the automorphism group of the network graph. Not all polysynchronous subspaces are robust; not all robust polysynchronous (synchrony) subspaces are fixed-point subspaces of symmetries. In fact, even for regular graphs, there are synchronies that do not come from symmetries of the graph automorphisms, and this has been named *exotic synchrony* by the authors in (ANTONELI; STEWART, 2006). We prove that, for homogeneous networks, all polysynchrony subspaces are generically robust polysynchronous (Theorem 3.3). Furthermore, we present two classes of regular graphs for which synchrony and symmetry coincide. One is the class of regular rings (any number of cells) and the other is the class of the so-called G_n -graphs ($5 \leq n \leq 9$ and $n = 11$); see Theorems 3.4 and 3.6. G_n is the graph of n cells connected by edges with nearest and next nearest neighbors. Subsection 5.4.2 presents the study of singularities of a Kuramoto network with coupling determined by the graph G_6 .

As the first step to extend the simple Kuramoto model, we characterize all vector fields whose Jacobian at any point is a Laplacian matrix (Theorem 5.6). We also deduce that these belong to a subset of gradient fields, namely those whose potential function operates on the differences between variables. In particular, it follows that the dynamics is completely understood from the study of critical points, from the LaSalle's principle of invariance. The results on stability of critical points then follows from an investigation of signs of the Laplacian matrix eigenvalues that can be deduced from Theorem 5.1. Yet based on the additive nature of Kuramoto systems, in Section 5.3 we impose an additive structure on the couplings. Under this condition, each component of the mapping being odd is a necessary condition (Theorem 5.10); for the Kuramoto network, this is the sine function. As an advantage, this structure provides a direct way to associate an admissible graph to this mapping, in a unique way, from the steps given in Chapter 4. This, in turn, enables us to use graph topology tools to study synchronization.

The authors in (JADBABAIE; MOTEE; BARAHONA, 2004) show that for the simple Kuramoto network the total synchrony is an asymptotically stable family of critical points. As our third main result, here we show that this also holds for the generalized Laplacian additive networks (Theorem 5.14). As mentioned above, the authors in (MANOEL; ROBERTS, 2015) describe the critical points on synchrony subspaces for gradient networks of identical cells on a ring with the additional condition of S^1 -invariance in the coupling function. We notice that these turn out to be a particular case of Laplacian additive networks; for the details we refer to (MANOEL; ROBERTS, 2015, Section 4). Here we present the complete list of critical points and their stability estimates for two examples of Laplacian additive network. As a first example, we consider a network with six identical cells with couplings determined by the regular network graph G_6 , with the coupling function to be the sine function as in the traditional Kuramoto model (Subsection 5.4.2). In the second example we consider a homogeneous network with six identical cells and two types of couplings, namely a combination of the sine and the identity functions.

This thesis is organized as follows. Chapter 2 is dedicated to presenting the basic concepts about coupled cell networks that we will need, and we present our first result (Proposition 2.4). In Chapter 3, we start to talk about synchronization on admissible vector fields in which we present conditions for an invariant subspace to be a synchrony subspace associated with the admissible network graph (Theorem 3.3). In this chapter, we also present two classes of network graphs without exotic balanced relations (Theorems 3.4 and 3.6). In Chapter 4, we describe a stepwise process to produce optimized network graphs for fixed vector fields, showing several examples. As our main results of this chapter, we classify them up to ODE-equivalence (Theorems 4.3 and 4.7). In Chapter 5, we present our study about the Laplacian map in which our main results are Theorems 5.9 and 5.10, which deal with the characterization of Laplacian maps, and Theorem 5.14, which establishes sufficient conditions for the asymptotic stability of total synchronization. We also present in Appendix A our lines of a code with the software *Wolfram Mathematica* that implements the algorithm given in (AGUIAR; DIAS, 2014). The results in Chapter 4 appear in (AMORIM; MANOEL, 2022, accepted in 14 November 2023 by *Nonlinearity*, IOP Publishing), accepted in 14 November 2023 by *Nonlinearity*, IOP Publishing. The results in Chapters 3 and 5 appear in (AMORIM; MANOEL, 2023).

COUPLED CELL NETWORKS

In this chapter we present the basic definitions and results of coupled cell networks and admissible maps that were introduced in (STEWART; GOLUBITSKY; PIVATO, 2003) for simple graphs and in (GOLUBITSKY; STEWART; TÖRÖK, 2005) these ideas was generalized for graphs with possible multi-arrows and loops (self-coupling). One of our results is also included here (Proposition 2.4).

2.1 Coupled Cell Networks

Cells are individual dynamical systems represented by vertices of a graph whose interactions are represented by the edges. A *coupled cell network* \mathcal{G} , with possible multiple couplings and self-couplings, consists of a finite set of cells $\mathcal{C} = \{1, \dots, n\}$ with an equivalence relation $\sim_{\mathcal{C}}$; a finite set of arrows (or edges) \mathcal{E} with an equivalence relation $\sim_{\mathcal{E}}$; two maps $\mathcal{H}, \mathcal{T} : \mathcal{E} \rightarrow \mathcal{C}$, where, for $e \in \mathcal{E}$, $\mathcal{H}(e)$ and $\mathcal{T}(e)$ are the head and the tail of e , with a compatibility condition,

$$e_1, e_2 \in \mathcal{E}, e_1 \sim_{\mathcal{E}} e_2 \Rightarrow \mathcal{H}(e_1) \sim_{\mathcal{C}} \mathcal{H}(e_2), \mathcal{T}(e_1) \sim_{\mathcal{C}} \mathcal{T}(e_2).$$

We shall also denote $\mathcal{G} = (\mathcal{C}, \mathcal{E}, \sim_{\mathcal{C}}, \sim_{\mathcal{E}})$. From now on, we shall also refer to a coupled cell network as a network graph. A self-coupling is an edge e such that $\mathcal{H}(e) = \mathcal{T}(e)$ and multiarrows are distinct edges e_1, e_2 such that $\mathcal{H}(e_1) = \mathcal{H}(e_2)$ and $\mathcal{T}(e_1) = \mathcal{T}(e_2)$. For a network graph \mathcal{G} with n cells, the order- n adjacency matrix of each type of edges $\xi \in \mathcal{E}/\sim_{\mathcal{E}}$ shall be denoted by $A_{\mathcal{G}}^{\xi}$ where

$$(A_{\mathcal{G}}^{\xi})_{ij} = |(\mathcal{T}^{-1}(j) \cap \mathcal{H}^{-1}(i) \cap \xi)|. \quad (2.1)$$

When it is clear from the context, we shall omit \mathcal{G} from this notation. For $c \in \mathcal{C}$, the *input set* of c is

$$I(c) = \{e \in \mathcal{E} : \mathcal{H}(e) = c\} = \mathcal{H}^{-1}(c).$$

The input equivalence relation $c \sim_I d$ between two cells $c, d \in \mathcal{C}$ is given by the existence of an arrow-type preserving bijection

$$\beta: I(c) \rightarrow I(d),$$

that is, $\beta(e) \sim_{\mathcal{E}} e$, for all $e \in I(c)$. The set of the input isomorphisms β is denoted by $B(c, d)$. The union of all $B(c, d)$ has a groupoid structure with respect to the composition. If $c \sim_I d$ and $I(c)$ is nonempty, then from the compatibility condition we have $c \sim_{\mathcal{E}} d$. Hence, if $I(c)$ is empty, then we require that $c \sim_I d$ implies $c \sim_{\mathcal{E}} d$.

Definition 2.1. A network graph \mathcal{G} is homogeneous if all cells are I -equivalent, in which case $B(c, d) \neq \emptyset$, for all $c, d \in \mathcal{C}$; and \mathcal{G} is regular if it is homogeneous with one type of edge.

An isomorphism between two network graphs $\mathcal{G}_1, \mathcal{G}_2$ is given in the natural way: if there exists a cell bijection $\gamma_{\mathcal{C}}: \mathcal{C}_1 \rightarrow \mathcal{C}_2$ and an arrow bijection $\gamma_{\mathcal{E}}: \mathcal{E}_1 \rightarrow \mathcal{E}_2$ such that

$$c \sim_{\mathcal{E}_1} d \Leftrightarrow \gamma_{\mathcal{C}}(c) \sim_{\mathcal{E}_2} \gamma_{\mathcal{C}}(d)$$

$$e \sim_{\mathcal{E}_1} e' \Leftrightarrow \gamma_{\mathcal{E}}(e) \sim_{\mathcal{E}_2} \gamma_{\mathcal{E}}(e')$$

$$\mathcal{T}_2(\gamma_{\mathcal{E}}(e)) = \gamma_{\mathcal{C}}(\mathcal{T}_1(e)), \mathcal{H}_2(\gamma_{\mathcal{E}}(e)) = \gamma_{\mathcal{C}}(\mathcal{H}_1(e)), \forall e \in \mathcal{E}_1.$$

Hence, \mathcal{G}_1 and \mathcal{G}_2 are isomorphic if, and only if, by a rearrangement of cells the adjacency matrices of \mathcal{G}_1 and \mathcal{G}_2 are the same. We denote by $Iso(\mathcal{G})$ the set of isomorphisms of \mathcal{G} into itself (see Corollary 4.8).

Remark 2.2. In a simple network graph (no multiple arrows), each arrow $e \in \mathcal{E}$ can be identified with the ordered pair $(\mathcal{T}(e), \mathcal{H}(e))$. In a network graph with no loops, for each arrow we have $\mathcal{T}(e) \neq \mathcal{H}(e)$. Hence, in the simple graph formalism, \mathcal{E} can be viewed as a subset of $\mathcal{C} \times \mathcal{C}$ with no elements of the form (c, c) , $c \in \mathcal{C}$ and the input set of $c \in \mathcal{C}$ can be viewed as the subset of \mathcal{C} given by $\{d \in \mathcal{C} \mid (d, c) \in \mathcal{E}\}$. Let us just point out that in (STEWART; GOLUBITSKY; PIVATO, 2003) it is assumed that $\{(c, c) \mid c \in \mathcal{C}\} \subset \mathcal{E}$ together with the condition that $(c, c) \sim_{\mathcal{E}} (d, d')$ holds only if $d' = d$ and $c \sim_{\mathcal{E}} d$, aiming to have in hand the useful condition that $c \in I(c)$. However, for formal purposes, this should be avoided, because an internal edge (c, c) can not be related to an external edge (d, d') , $d \neq d'$.

2.2 Admissible vector fields

For each cell $c \in \mathcal{C}$, let P_c denote its domain, or the so-called *cell phase space*, which is a nontrivial finite-dimensional real vector space. We require

$$c \sim_{\mathcal{E}} d \Rightarrow P_c = P_d, \tag{2.2}$$

in which case we use the same coordinate system for P_c and P_d . The *total phase space* and the *coupled phase space* of $c \in \mathcal{C}$ are, respectively,

$$P = \prod_{c \in \mathcal{C}} P_c, \quad P_{I(c)} = \prod_{e \in I(c)} P_{\mathcal{F}(e)}, \quad (2.3)$$

the coordinate system of the later being $y = (y_e)_{e \in I(c)}$. Consider now the map

$$\begin{aligned} \pi_{I(c)}: \quad P &\longrightarrow P_{I(c)} \\ x = (x_{c'})_{c' \in \mathcal{C}} &\longmapsto \pi_{I(c)}(x) = (x_{\mathcal{F}(e)}) \end{aligned},$$

which repeats each variable $x_{c'}$ as many times as the number of edges from c' to c in $I(c)$. In particular, from (2.2) it follows that, if $c \sim_I d$, then $P_{I(c)} = P_{I(d)}$.

Finally, for any $c \in \mathcal{C}$, the vertex group $B(c, c)$ has a natural action on $P_{I(c)}$ as follows: for each $\beta \in B(c, c)$ we have the *pullback* map

$$\beta^*: P_{I(c)} \rightarrow P_{I(c)}$$

defined by

$$\beta^*(y)_e = y_{\beta(e)}, \quad \forall e \in I(c).$$

Similarly, for $\beta \in B(c, d)$, we also define $\beta^*: P_{I(d)} \rightarrow P_{I(c)}$. We can now recall the concept of admissible vector field:

Definition 2.3. A vector field $f: P \rightarrow P$ is \mathcal{G} -admissible if the following hold:

- (a) *Domain condition:* For all $c \in \mathcal{C}$, the component f_c depends only on the internal phase space; that is, there exists $\hat{f}_c: P_c \times P_{I(c)} \rightarrow P_c$ such that

$$f_c(x) = \hat{f}_c(x_c, \pi_{I(c)}(x)). \quad (2.4)$$

- (b) *Pullback condition:* For any pair $c, d \in \mathcal{C}$ and $\beta \in B(c, d)$,

$$\hat{f}_d(x_d, y) = \hat{f}_c(x_d, \beta^*(y)) \quad \forall (x_d, y) \in P_d \times P_{I(d)}. \quad (2.5)$$

We notice that when $c = d$ the pullback condition means that \hat{f}_c is $B(c, c)$ -invariant in the y -variable. In this case, we write

$$\overline{\hat{f}_c(x_c, y_1^1, \dots, y_{|I(c) \cap \xi_1|}^1, \dots, y_1^r, \dots, y_{|I(c) \cap \xi_r|}^r)}, \quad (2.6)$$

where over bar means invariance under the permutations of these variables.

We denote by $\mathcal{F}(\mathcal{G}; P)$ the set of smooth \mathcal{G} -admissible vector fields on P , and by $\mathcal{L}(\mathcal{G}; P)$ the set of linear \mathcal{G} -admissible vector fields on P . We finish this subsection with the following characterization, which is straightforward and shall be very useful in the sequel:

$$\mathcal{L}(\mathcal{G}; \mathbb{R}^n) = \left\{ \text{diag}(t_1, \dots, t_n) + \sum_{\xi \in \mathcal{E}/\sim_{\mathcal{E}}} \text{diag}(t_1^\xi, \dots, t_n^\xi) A_{\mathcal{G}}^\xi : i \sim_I j \Rightarrow t_i = t_j, t_i^\xi = t_j^\xi \right\}. \quad (2.7)$$

2.3 ODE-equivalence

Topologically distinct network graphs can determine the same space of smooth admissible vector fields. This statement is precisely the notion of *ODE-equivalence* between network graphs (see (DIAS; STEWART, 2005)). It turns out that verifying the ODE-equivalence can be reduced to the linear level. In fact, as established in (DIAS; STEWART, 2005, Theorem 5.1, Corollary 7.7), two network graphs \mathcal{G}_1 and \mathcal{G}_2 of n cells are ODE-equivalent if, and only if, there exists an input-preserving bijection $\gamma: \mathcal{C}_1 \rightarrow \mathcal{C}_2$ such that

$$\mathcal{L}(\mathcal{G}_1; \mathbb{R}^n) = \gamma^T \mathcal{L}(\mathcal{G}_2; \mathbb{R}^n) \gamma. \quad (2.8)$$

It is direct from (2.7) that if \mathcal{G}_1 and \mathcal{G}_2 are isomorphic, then they are ODE-equivalent. Our first result claims that the converse holds for the homogeneous simple case:

Proposition 2.4. *Let \mathcal{G}_1 and \mathcal{G}_2 be homogeneous simple network graphs. If \mathcal{G}_1 and \mathcal{G}_2 are ODE-equivalent, then they are isomorphic.*

Proof. Let $\gamma: \mathcal{C}_1 \rightarrow \mathcal{C}_2$ be a bijection that realizes the ODE-equivalence (2.8). Since each graph is simple, if a position of any of its adjacency matrix is 1, then the same position in all the other of its adjacency matrices is zero. In particular, the adjacency matrices of a simple graph are linearly independent. Hence, from (2.7), \mathcal{G}_1 and \mathcal{G}_2 have the same number of adjacency matrices. For simplicity, suppose this number is 2 and let $A_{\mathcal{G}_1}^k$ and $A_{\mathcal{G}_2}^k$, $k = 1, 2$, be their adjacency matrices.

Let s^1, s^2 be such that

$$A_{\mathcal{G}_1}^1 = s^1 (\gamma^T A_{\mathcal{G}_2}^1 \gamma) + s^2 (\gamma^T A_{\mathcal{G}_2}^2 \gamma).$$

Now, let (i, j) be such that $(A_{\mathcal{G}_1}^1)_{ij} = 1$. Without loss of generality, we can assume that

$$(\gamma^T A_{\mathcal{G}_2}^1 \gamma)_{ij} = 1 \text{ and } (\gamma^T A_{\mathcal{G}_2}^2 \gamma)_{ij} = 0.$$

Hence,

$$A_{\mathcal{G}_1}^1 = (\gamma^T A_{\mathcal{G}_2}^1 \gamma) + s^2 (\gamma^T A_{\mathcal{G}_2}^2 \gamma). \quad (2.9)$$

But $(A_{\mathcal{G}_1}^2)_{ij} = 0$. It then follows that

$$A_{\mathcal{G}_1}^2 = (\gamma^T A_{\mathcal{G}_2}^2 \gamma),$$

and then $s^2 = 0$ in (2.9). So the result follows. \square

The proposition above is very useful to deduce the complete list of distinct non equivalent admissible graphs of a given vector field for the homogeneous simple case. See the case study of Subsection 4.5.

SYNCHRONY AND SYMMETRY

Subspaces that remain unchanged under the dynamics hold significance. This chapter focuses on synchrony patterns, as they constitute subspaces of dynamics invariance in the network context and how they emerge from symmetry. Existence of symmetries and synchronies force existence of invariant subspaces, because of their fixed-point sets and robustly polysynchronous subspaces, respectively. These are related notions and we now turn to the issue of synchronies with respect to symmetries of a network graph. The results in this Chapter appear in (AMORIM; MANOEL, 2023).

We initiate by briefly revisiting the fundamental concepts.

In broad terms, synchrony is a natural concept in network dynamics related to a partition of the cells into subsets (often called clusters) such that all cells in the same cluster are synchronous. In a network system, that is, a system of ordinary differential equations

$$\dot{x} = f(x), \quad x \in P, \quad (3.1)$$

where $f \in \mathcal{F}(\mathcal{G}; P)$ and P is as in (2.3), synchrony occurs when two or more cells of a solution $x(t)$ behave identically, that is, if c and d are any two of these cells, then

$$x_c(t) = x_d(t), \quad \forall t \in D,$$

where D is a domain in \mathbb{R} for which $x(t)$ exists. The authors in (GOLUBITSKY; STEWART; TÖRÖK, 2005; STEWART; GOLUBITSKY; PIVATO, 2003) characterize occurrence of synchrony in a network dynamics from the graph architecture. This is given as follows.

Let \bowtie be an equivalence relation on \mathcal{C} . Then

- \bowtie is said to be *balanced* if $c \bowtie d$ implies that there exists $\beta \in B(c, d)$ such that $\mathcal{T}(e) \bowtie \mathcal{T}(\beta(e)), \forall e \in I(c)$;

- \bowtie is *robustly polysynchronous* if for any choice of total phase space P we have $f(\Delta_{\bowtie}) \subseteq \Delta_{\bowtie}$, for all $f \in \mathcal{F}(\mathcal{G}, P)$, where

$$\Delta_{\bowtie} = \{x \in P \mid x_c = x_d \Leftrightarrow c \bowtie d\}.$$

We notice that the first of the notions above is associated with the graph \mathcal{G} , whereas the second is related to the vector space $\mathcal{F}(\mathcal{G}, P)$, but it turns out that both notions are equivalent, as established in (GOLUBITSKY; STEWART; TÖRÖK, 2005, Theorem 4.3). Moreover, the authors prove that these are also equivalent to

$$A_{\mathcal{G}}^{\xi}(\Delta_{\bowtie}) \subseteq \Delta_{\bowtie}, \quad \forall \xi \in \mathcal{E}/\sim_{\mathcal{G}}, \quad \text{when } P = \mathbb{R}^n, \quad (3.2)$$

that is, synchrony subspaces of \mathbb{R}^n are those left invariant under all adjacency matrices of \mathcal{G} .

Definition 3.1. *When \bowtie is balanced, Δ_{\bowtie} is called a synchrony subspace.*

The practical way to express the resulting \bowtie -classes of a synchrony pattern is coloring vertices: cells in the same class have the same color and ‘receive from edges’ vertices of the same color.

Remark 3.2. Based on (3.2), the authors in (AGUIAR; DIAS, 2014) develop, for a given network graph, an algorithm whose output is the set of synchrony subspaces. This is done through polydiagonal invariant subspaces from the eigenvectors of the Jordan decomposition of the adjacency matrices. As they show, it suffices to implement the algorithm for the case of regular graph, because all the lattice of synchrony subspaces can be associated with a regular network through the notion they introduce of *minimal synchrony subspaces that are sum-irreducible*. Following this approach, we have implemented this algorithm with a code using the software *Mathematica*. The code has been useful to compute the synchrony patterns presented in this work. This code is included here as Appendix A.

3.1 Synchronies from invariant subspaces

In this subsection we relate synchrony subspaces of a network graph \mathcal{G} to invariant subspaces under the dynamics of (3.1) for $f \in \mathcal{F}(\mathcal{G}; P)$.

Theorem 3.3. *For any homogeneous network graph \mathcal{G} on any phase space P , polydiagonal subspaces of P that are invariant under an generic admissible vector field are synchrony subspaces.*

Proof. Based on (3.2) we assume, without loss of generality, that each cell phase space is one dimensional, so $P = \mathbb{R}^n$, where n is the number of cells. Since \mathcal{G} is homogeneous, the Jacobian of an admissible map f at any point of total synchrony $\mathbf{v} = (t, \dots, t) \in \mathbb{R}^n$ is

$$Jf(\mathbf{v}) = a(\mathbf{v})I + \sum_{\xi \in \mathcal{E}/\sim_{\mathcal{G}}} b^{\xi}(\mathbf{v})A^{\xi}, \quad (3.3)$$

where A^ξ are the adjacency matrices of \mathcal{G} . Let $\Theta \subset \mathbb{R}^n$ be polydiagonal such that $f(\Theta) \subset \Theta$. As $\mathbf{v} \in \Theta$ then $Jf(\mathbf{v})[\Theta] \subset \Theta$, that imply

$$\sum_{\xi \in \mathcal{E}/\sim_{\mathcal{E}}} b^\xi(\mathbf{v}) A^\xi[\Theta] \subset \Theta.$$

If there are $\mathbf{v}^1, \mathbf{v}^2, \dots, \mathbf{v}^{|\mathcal{E}/\sim_{\mathcal{E}}|}$ such that

$$\det[b^i(\mathbf{v}^j)] \neq 0 \quad (\text{generic condition}),$$

then $A^\xi[\Theta] \subset \Theta, \forall \xi \in \mathcal{E}/\sim_{\mathcal{E}}$ and (3.2) concludes the proof. \square

In Subsection 5.4.2 we investigate existence and nature of singularities inside synchrony subspaces. For the ODE (5.15), it is straightforward that $b(\mathbf{v}) = 1$, for any $\mathbf{v} \in \mathbb{T}^n$, so the singularities we find are in fact all the possible equilibria inside invariant subspaces, by Theorem 3.3.

3.2 Synchrony and symmetry in regular networks

A symmetry of \mathcal{G} , or an automorphism of \mathcal{G} , is a isomorphism itself such that $e \sim_{\mathcal{E}} \gamma_{\mathcal{E}}(e)$. The group $\text{Aut}(\mathcal{G})$ of all such automorphisms is the symmetry group of \mathcal{G} . It is well known that symmetries of a network graph determine synchronies, for every subgroup $\Sigma < \text{Aut}(\mathcal{G})$ defines a balanced equivalence relation on \mathcal{G} ((ANTONELI; STEWART, 2006, Proposition 3.3)):

$$c \bowtie_{\Sigma} d \Leftrightarrow \exists \gamma \in \Sigma : \gamma_{\mathcal{E}}(c) = d.$$

This is the same as saying that the synchrony subspace $\Delta_{\bowtie_{\Sigma}}$ is the fixed-point subspace of Σ ,

$$\text{Fix}(\Sigma) = \{x \in P : \sigma x = x, \forall \sigma \in \Sigma\}.$$

As it is also well known, the converse does not hold in general; that is, not all synchrony subspaces are fixed-point subspaces. Such synchrony has been named an *exotic* synchrony after (ANTONELI; STEWART, 2006). A balanced relation \bowtie is called *exotic* if there is no subgroup $\Sigma < \text{Aut}(\mathcal{G})$ for which $\bowtie = \bowtie_{\Sigma}$.

Exotic patterns can appear in homogeneous graphs and even in the most simple cases of regular graphs. The first example in the literature was presented in (GOLUBITSKY; NICOL; STEWART, 2004), the regular graph G_{12} of twelve vertices with nearest and next nearest neighbors. In Table 2 of chapter 4 we show seven homogeneous network graphs #2 – #8 presenting exotics patterns.

There are however classes of network graphs for which all synchronies are determined by the symmetries of \mathcal{G} . For example, the regular network graph G_6 of six cells with nearest and next nearest neighbor coupling of Subsection 5.4.2, which falls in the set of graphs given in Theorem 3.6. The next proposition states that this is also the case for the regular ring of n cells

with nearest neighbor coupling, for which $\text{Aut}(\mathcal{G}) = \mathbb{D}_n$. Although the result is not surprising, the proof is not straightforward and, to our knowledge, it has not been found in the literature, so it is included here.

Theorem 3.4. *There are no exotic pattern of synchrony for the regular ring of n cells, with nearest neighbor coupling, for $n \geq 3$.*

Proof. If \bowtie is a balanced equivalence relation, we prove that $\bowtie = \bowtie_\Sigma$ for some subgroup $\Sigma < \mathbb{D}_n$.

The following is a necessary condition for the equivalence relation \bowtie to be balanced for this network graph:

$$c \bowtie d \Rightarrow \begin{cases} (c-1 \bowtie d-1, c+1 \bowtie d+1) \\ \text{or} \\ (c-1 \bowtie d+1, c+1 \bowtie d-1). \end{cases} \quad (3.4)$$

First, suppose that there are three consecutive \bowtie -equivalent cells. By (3.4), all cells must be \bowtie -equivalent, and so $\bowtie = \bowtie_{\mathbb{D}_n}$.

We now suppose $c \bowtie d$ such that

$$c-1 \bowtie d-1, c+1 \bowtie d+1. \quad (3.5)$$

We need to identify Δ_{\bowtie} as a fixed-point subspace of a subgroup $\Sigma < \mathbb{D}_n$, that is, find a rotation multiple of $2\pi/n$ or a line reflection generating Σ .

We can assume that $d-c > 0$ is minimal with respect to (3.5). There is a sequence of \bowtie -classes with length $d-c$ that repeats inside the ring. In fact, by (3.4),

$$c \bowtie d, c+1 \bowtie d+1 \Rightarrow c+2 \bowtie d+2 \Rightarrow \dots \Rightarrow c+(d-c) = d \bowtie d+(d-c).$$

Hence, $d-c$ divides n and then a rotation of $2(d-c)\pi/n$ is a generator of Σ .

Finally, suppose that there are two cells $c' \bowtie d'$ such that $c < c' < d' < d$ and by minimality of $d-c > 0$ we have that $c'-1 \bowtie d'+1, c'+1 \bowtie d'-1$. The line reflection that takes c' into d' also takes $c'-1$ into $d'+1, c'+1$ into $d'-1$ and so on. Then, this reflection is a generator of Σ . \square

Remark 3.5. A study of a gradient network of identical oscillators on a ring is carried out in (MANOEL; ROBERTS, 2015). We notice that in the description given in (MANOEL; ROBERTS, 2015, Table 1) a symmetry in one type of critical points in that table is missing. In fact, inside their list of critical points with trivial isotropy, there is a subclass with nontrivial isotropy, namely $\mathbb{Z}_2 < \mathbb{D}_n$, which is supported by Theorem 3.4 above. Nonetheless, we point out that this does not affect the list of all possible critical points presented in that table, which is in fact complete.

The following result gives another set of regular network graphs for which all synchronies are symmetries:

Theorem 3.6. *There are no exotic pattern of synchrony for the network graph G_n , for $5 \leq n \leq 9$ and $n = 11$.*

Proof. This follows by an extensive use of the *Mathematica* code; see Remark 3.2. □

The list of exotic patterns of G_{10} is given in (ANTONELI; STEWART, 2006, Section 7), which we have confirmed with our code. The network graph G_{12} presents an exotic pattern, as already mentioned above. Due to the computational complexity, we have not investigated existence of exotic patterns in G_n for $n \geq 13$ yet. Some attempts suggest that there may be a general procedure to answer the question for bigger n and we intend to go in this direction as a near future work.

THE REALIZATION OF ADMISSIBLE GRAPHS FOR COUPLED VECTOR FIELDS

As recalled in Chapter 2, based on the action of a groupoid of symmetries of a given network graph, the authors in (GOLUBITSKY; STEWART; TÖRÖK, 2005) and (STEWART; GOLUBITSKY; PIVATO, 2003) formulate in algebraic terms the class of admissible vector fields on the total phase space that are ‘compatible’ with the labeled structure of a given graph. In this section we follow that formulation to study the problem in the inverse direction. We give the procedure to construct the network graphs associated with a given vector field, namely the admissible graphs for this vector field. The results in this Chapter appear in (AMORIM; MANOEL, 2022, accepted in 14 November 2023 by *Nonlinearity*, IOP Publishing).

Before that, we point out that permutations play a major role in the two directions. Let us illustrate the two approaches together, with the elementary graphs of Fig. 2. The general admissible vector field for the network graph on the left is of the form

$$\begin{aligned} \dot{x}_1 &= f(x_1, x_2, x_3) \\ \dot{x}_2 &= g(x_2, x_1) \\ \dot{x}_3 &= h(x_3, x_1), \end{aligned}$$

for any three-variable function f and two-variable functions g and h . But it should be reasonable to go on with the analysis assuming an additional necessary condition, namely f non invariant under the permutation of x_2 and x_3 (together with g and h distinct), in the same way that this permutation invariance is a necessary condition for the above vector field to be admissible for the network graph on the right (together with $g = h$). For the inverse problem, the possible (and not possible) permutation invariances can be taken into account in the initial process of constructing the graphs, soon after the choice of the number of vertices. In fact, this is the basis for the stepwise procedure of Subsection 4.1 to produce admissible graphs, as well as ‘optimized’ admissible graphs as a final step. By an optimized admissible graph we mean a graph that indeed depicts the permutation invariances of the components of this vector field with the least number

of edge types. In the broad sense of admissibility, any vector field yields an admissible graph, for we can take the complete graph with all edges in distinct classes for example. However, this graph has no nontrivial symmetries and should not be of much interest if we are to model many features of coupled dynamics such as synchronization.



Figure 2 – (a) A 3-cell graph with distinct couplings and (b) a 3-cell graph with identical couplings.

4.1 The stepwise procedure

For a given C^1 vector field, this is a step-by-step procedure to give the complete list of admissible graphs, up to ODE-equivalence. It is also an optimization method of choosing systematically input values from within an allowed set from the mapping components. The general idea is: compare the components according to (2.5); by comparison, define the equivalence relation $\sim_{\mathcal{C}}$ of vertices and also the equivalence relations \sim_k of edges in four steps, $k = 1, 2, 3, 4$. The relation $\sim_{\mathcal{C}}$ is established in step 1. For $k = 2, 3, 4$, the relation \sim_k is constructed in the k^{th} step and its classes are obtained by joining classes of \sim_{k-1} .

Let $f \in C^1(\mathbb{R}^n; \mathbb{R}^n)$ be a given vector field.

Step 1. Choose the number of cells n_0 , $\mathcal{C} = \{1, \dots, n_0\}$. The natural choice is $n_0 = n$, in which case each cell domain is $P_c = \mathbb{R}$. If $n_0 < n$, then this naturally involves other choices, namely of the cell domains. From the definition of admissible vector field, the relation $\sim_{\mathcal{C}}$ must indicate the compatibility between cell domains; hence, the coarsest relation $\sim_{\mathcal{C}}^0$ we can define on \mathcal{C} is

$$c \sim_{\mathcal{C}}^0 d \iff P_c = P_d,$$

for $P_1 \times \dots \times P_{n_0} = \mathbb{R}^n$, $P_c \neq \{0\}$, $\forall c \in \mathcal{C}$. Let $\sim_{\mathcal{C}}$ be a refinement of or equal to $\sim_{\mathcal{C}}^0$ on \mathcal{C} , that is,

$$c \sim_{\mathcal{C}} d \implies c \sim_{\mathcal{C}}^0 d.$$

An edge from a vertex d to a vertex c in an admissible graph shall represent that ‘ c depends on d ’. However, posing this condition may not be a simple task when we consider multiarrows. The procedure is supported by the following two mappings:

For each $c \in \mathcal{C}$, consider the canonical submersion

$$\pi_c : \mathbb{R}^n \longrightarrow \prod_{d=1}^{n_0} (P_d)^{m_{cd}} \quad (4.1)$$

$$x \longmapsto (\dots, \overbrace{x_d, \dots, x_d}^{m_{cd} \text{ times}}, \dots), \quad (4.2)$$

which indicates how the variable x_d repeats and the number m_{cd} of this repetition. Also, for the c -component of f , f_c , we consider an associated generating function

$$\hat{f}_c: P_c \times \prod_{d=1}^{n_0} (P_d)^{m_{cd}} \rightarrow P_c \quad (4.3)$$

such that

$$\frac{\partial \hat{f}_c}{\partial y_e} \neq 0,$$

for any variable y_e of \hat{f}_c , and

$$f_c(x) = \hat{f}_c(x_c, \pi_c(x)), \forall x \in P.$$

Thus, the number of arrows from d to c is m_{cd} . The simplest choice is to consider, for every $c \in \mathcal{C}$, only the variables such that $\partial f_c / \partial x_d \neq 0$ and each x_d appearing once in π_c . This yields $\hat{f}_c = f_c$, and the resulting graph is a simple graph.

With respect to the set \mathcal{E} of edges, we now establish the equivalence relation \sim_1 . In this step, we take all edges in distinct classes, that is, $B_1(c, c)$ is trivial and $B_1(c, d)$ is empty if $c \neq d$ and, therefore, the equivariance condition is trivially satisfied. At this point we have the relations $\sim_{\mathcal{C}}$ for cells and \sim_1 for edges. Let \mathcal{G}_1 denote such network graph.

Step 2. For each $c \in \mathcal{C}$, take the unique partition of $I(c)$,

$$I(c) = (K^1 := \{e_1^1(c), \dots, e_{s_1}^1(c)\}) \dot{\cup} \dots \dot{\cup} (K^r := \{e_1^r(c), \dots, e_{s_r}^r(c)\}), \quad (4.4)$$

such that \hat{f}_c is invariant under all permutations of $y_{e_{s_{r'}}^1}, \dots, y_{e_{s_{r'}}^r}$, for all $r' = 1, \dots, r$. Each $K_{r'}$ is contained in a $\sim_{\mathcal{C}}$ -class and it is maximal with respect to these proprieties. Consequently, r is minimal. Hence, by this construction, f_c is invariant under the group $\mathbf{S}_{s_1} \times \dots \times \mathbf{S}_{s_r}$. From this, we define the equivalent relation \sim_2 on \mathcal{E} ,

$$e_k^i \sim_2 e_l^j \Leftrightarrow i = j.$$

In this way, $B(c, c) = \mathbf{S}_{s_1} \times \dots \times \mathbf{S}_{s_r}$ and $B(c, d)$ is empty.

Step 3. Construct an input equivalence relation, for which we use again the notation \sim_I , and an equivalence relation \sim_3 on \mathcal{E} . Here the components of the vector field are compared. For distinct $c, d \in \mathcal{C}$, $c \sim_{\mathcal{C}} d$, consider the partitions as in (4.4) constructed in step 2,

$$\begin{aligned} I(c) &= \{e_1^1(c), \dots, e_{s_1}^1(c)\} \dot{\cup} \dots \dot{\cup} \{e_1^r(c), \dots, e_{s_r}^r(c)\}, \\ I(d) &= \{e_1^1(d), \dots, e_{q_1}^1(d)\} \dot{\cup} \dots \dot{\cup} \{e_1^p(d), \dots, e_{q_p}^p(d)\}. \end{aligned}$$

If $r = p$, $s_i = q_i$, $\forall i = 1, \dots, r$, and

$$\hat{f}_c(x_c, \overline{y_{e_1^1(c)}}, \dots, \overline{y_{e_{s_1}^1(c)}}), \dots, \overline{y_{e_1^r(c)}}, \dots, \overline{y_{e_{s_r}^r(c)}}) = \hat{f}_d(x_c, \overline{y_{e_1^1(d)}}, \dots, \overline{y_{e_{s_1}^1(d)}}), \dots, \overline{y_{e_1^r(d)}}, \dots, \overline{y_{e_{s_r}^r(d)}}) \quad (4.5)$$

define the equivalence relation \sim_3 on \mathcal{E} ,

$$e_k^i(c) \sim_3 e_l^j(d) \Leftrightarrow i = j, \quad (4.6)$$

which gives the input equivalence $c \sim_I d$. On the other hand, if either $r \neq p$ or $s_i \neq q_i$ for some i , or if (4.5) is not satisfied, then c can not be input-equivalent to d .

Step 4. Construct \sim_4 . From the input equivalence relation obtained in step 3, if $c \not\sim_I d$, then $e(c) \sim_4 e'(d)$ has no effect from the point of view of the vector field, except that $c \sim_{\mathcal{E}} d$. Therefore, edges can be attributed to the same \sim_4 -class as long as the input equivalence classes are unchanged. This attribution provides further reduction on the number of classes of step 3.

Remark 4.1. (a) Each I -class Q determines uniquely the natural numbers $r =: r(Q), s_1, \dots, s_r$ in (4.5).

(b) The relation (4.5) may not be uniquely satisfied. This is the case if for example a generating function \hat{f}_c is setwise invariant: suppose that $s_u = s_v$ and

$$\hat{f}_c(\dots, \overline{y_{e_1^u}}, \dots, \overline{y_{e_{s_u}^u}}, \dots, \overline{y_{e_1^v}}, \dots, \overline{y_{e_{s_v}^v}}, \dots) = \hat{f}_c(\dots, \overline{y_{e_1^v}}, \dots, \overline{y_{e_{s_v}^v}}, \dots, \overline{y_{e_1^u}}, \dots, \overline{y_{e_{s_u}^u}}, \dots), \quad (4.7)$$

for some $1 \leq u, v \leq r$, that is, the two sets K^u and K^v can be interchanged in the component f_c . In this case, there are two possible choices in (4.5) and, therefore, two choices for (4.6). More generally, for each I -class Q , there may exist $c \in Q$ such that the collection $\{K^1, \dots, K^r\}$ in (4.4) can be partitioned into sets

$$\{K^1, \dots, K^{u_1}\}, \{K^{u_1+1}, \dots, K^{u_1+u_2}\}, \dots, \{K^{u_1+\dots+u_{v-1}+1}, \dots, K^{u_1+\dots+u_v}\}, \quad (4.8)$$

where $u_1 + \dots + u_v = r$, such that \hat{f} is invariant by permutation among the sets $K^{u_1+\dots+u_{t-1}+1}, \dots, K^{u_1+\dots+u_t}$, for all $t = 1, \dots, v$. In particular,

$$|K^{u_1+\dots+u_{t-1}+1}| = \dots = |K^{u_1+\dots+u_t}|, \quad t = 1, \dots, v. \quad (4.9)$$

This remark also yields Proposition 4.2, which gives an upper bound for the number of admissible graphs for a vector field.

(c) The graphs of step 4 are optimized graphs, in the sense that they contemplate all the permutation invariances of the components of the vector field with the least number of edge types.

(d) As expected, the groupoid of symmetries of the graphs obtained in step 4 may not comprise all the symmetries in the components of f . In fact, these extra symmetries may lead to distinct ODE-classes of admissible graphs (see Theorem 4.3).

4.2 Example: a vector field on \mathbb{R}^4

Consider the vector field f on \mathbb{R}^4 whose components are

$$\begin{aligned} f_1(x_1, x_2, x_3, x_4) &= x_1x_2 + x_3x_4 \\ f_2(x_1, x_2, x_3, x_4) &= x_1x_2x_3x_4 \\ f_3(x_1, x_2, x_3, x_4) &= x_3x_4 + x_1x_2 \\ f_4(x_1, x_2, x_3, x_4) &= x_1x_2x_3x_4. \end{aligned} \tag{4.10}$$

As we shall see, this vector field admits admissible simple graphs with four, three and two cells.

4 cells. Step 1: The number of cells is the domain dimension. So $\mathcal{C} = \{1, 2, 3, 4\}$. Since for all $i, j = 1, \dots, 4$ $\partial f_i / \partial x_j$ is not identically zero, there must be an edge from any vertex to any other vertex, so $\mathcal{E} = \mathcal{C} \times \mathcal{C}$. The network graph \mathcal{G}_1 is then the simple complete graph with 12 possibly distinct arrows. Step 2: Starting with f_1 , x_1 is the distinguished variable, so the unique permutation invariance is over the variables x_3 and x_4 , so $(3, 1) \sim_2 (4, 1)$. For f_2 , x_2 is the distinguished variable and f_2 is invariant under permutation over x_1, x_3 and x_4 , so $(1, 2) \sim_2 (3, 2) \sim_2 (4, 2)$. Similar constructions hold for f_3 and f_4 , respectively. Hence,

$$I(1) = \{2\} \cup \{3, 4\}, \quad I(2) = \{1, 3, 4\}, \quad I(3) = \{4\} \cup \{1, 2\}, \quad I(4) = \{1, 2, 3\},$$

and the vertex groups are $B(1, 1), B(3, 3)$ isomorphic to $S_1 \times S_2 \simeq S_2$ and $B(2, 2), B(4, 4)$ isomorphic to S_3 . The graph is \mathcal{G}_2 given in Fig. 3, with six \sim_2 -classes. Step 3: This is the correlation among components and we have that $1 \sim_2 3 \not\sim_2 2 \sim_2 4$. It then follows that the new graph \mathcal{G}_3 is given in Fig 4, with three \sim_3 -classes. Step 4: Up to input equivalence, \sim_3 can be refined in two distinct ways. In fact, $1 \sim_I 3 \approx_I 2 \sim_I 4$, so the edges between vertices 1 and 2 (or 3 and 4) can be taken in distinct edge classes (graph \mathcal{G}_4^1 in Fig. 5) or in the same edge class (graph \mathcal{G}_4^2 in Fig. 5).

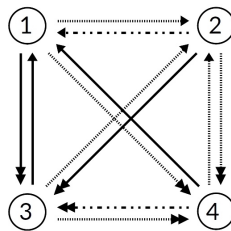


Figure 3 – Admissible graph \mathcal{G}_2 for (4.10) with six \sim_2 -classes.

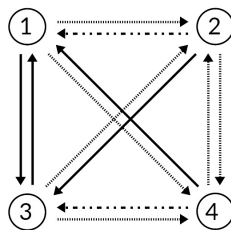


Figure 4 – Admissible graph \mathcal{G}_3 for (4.10) with three \sim_3 -classes.

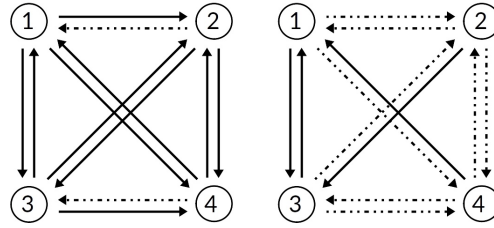


Figure 5 – Admissible graphs \mathcal{G}_4^1 (left) and \mathcal{G}_4^2 (right) for (4.10) with two \sim_4 -classes.

3 cells. Step 1: Choose the cell domains to be $P_1 = \mathbb{R}^2$ with coordinates $y_1 = (x_1, x_2)$, and $P_2 = \mathbb{R}$, $P_3 = \mathbb{R}$ with coordinates $y_2 = x_3$, $y_3 = x_4$, respectively. So $\mathcal{C} = \{1, 2, 3\}$ and the \mathcal{C} -classes are $\{1\}$ and $\{2, 3\}$. Rewrite (4.10) as

$$g_1(y_1, y_2, y_3) = (x_1x_2 + x_3x_4, x_1x_2x_3x_4)$$

$$g_2(y_1, y_2, y_3) = x_1x_2 + x_3x_4$$

$$g_3(y_1, y_2, y_3) = x_1x_2x_3x_4.$$

In step 2, we obtain the graph of Fig. 6. Regarding the vertex groups, we have $B(1, 1) \simeq \mathbf{S}_2$. Also, $I(2)$ is formed by two arrows of different types, so these can not be permuted and the unique bijection of $B(2, 2)$ is the identity. The same goes for $I(3)$. Hence, $B(2, 2) \simeq B(3, 3) \simeq \{I\}$. Step 3 gives the three I -classes $\{1\}, \{2\}, \{3\}$. And moving to step 4, only one graph is deduced, by $(2, 3) \sim_{\mathcal{E}} (3, 2)$; see Fig 7.

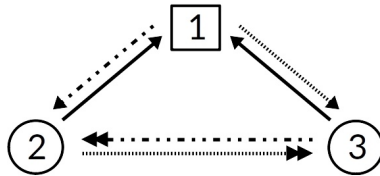


Figure 6 – An admissible graph \mathcal{G}_2 for (4.10) seen as a network of 3 cells.

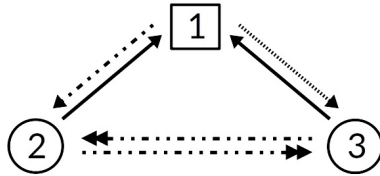


Figure 7 – An admissible graph \mathcal{G}_4 for (4.10) seen as a network of 2 cells.

2 cells: In this case, we choose the cell phase spaces $P_1 = \mathbb{R}^2$ with coordinate $y_1 = (x_1, x_2)$ and $P_2 = \mathbb{R}^2$ with coordinate $y_2 = (x_3, x_4)$ and rewrite (4.10) as

$$h_1(y_1, y_2) = (f_1, f_2) = (x_1x_2 + x_3x_4, x_1x_2x_3x_4)$$

$$h_2(y_1, y_2) = (f_3, f_4) = (x_1x_2 + x_3x_4, x_1x_2x_3x_4).$$

Clearly the optimized admissible graph for this network is as in Fig. 8.

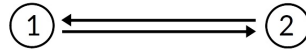


Figure 8 – An admissible graph \mathcal{G}_4 for (4.10) seen as a network of 2 cells.

4.3 Simple graph versus multigraph

In this section we finish the discussion of regarding the ODE given in (1.1) started in the Introduction: we construct the possible network graphs using the procedure of Subsection 4.1 for the vector field on \mathbb{R}^3 with components

$$\begin{aligned} f_1(x_1, x_2, x_3) &= x_1 + x_1^3 \\ f_2(x_1, x_2, x_3) &= x_2 + x_2^2 x_3 \\ f_3(x_1, x_2, x_3) &= x_3 + x_1 x_2 x_3. \end{aligned} \quad (4.11)$$

Simple graph. Step 1: we have that $\mathcal{C} = \{1, 2, 3\}$ with valencies 0, 1, 2 and it makes it consistent to take $1 \not\sim_I 2 \not\sim_I 3 \not\sim_I 1$. Step 2: this leads easily to $(1, 3) \sim_2 (2, 3)$. The input and the edges equivalences are unchanged in step 3. Step 4: this leads easily to $(1, 3) \sim_4 (2, 3) \sim_4 (3, 2)$, producing an optimized simple graph; see Fig. 1 (left).

Multigraph. The function $\hat{f}_c : \mathbb{R}^4 \rightarrow \mathbb{R}$,

$$\hat{f}_c(x, \overline{y_1, y_2, y_3}) = x + y_1 y_2 y_3$$

is a generating function of all components f_c , $c = 1, 2, 3$, in (4.11),

$$\begin{aligned} f_1(x_1, x_2, x_3) &= \hat{f}_1(x_1, \overline{x_1, x_1, x_1}) \\ f_2(x_1, x_2, x_3) &= \hat{f}_2(x_2, \overline{x_2, x_2, x_3}) \\ f_3(x_1, x_2, x_3) &= \hat{f}_3(x_3, \overline{x_1, x_2, x_3}). \end{aligned} \quad (4.12)$$

Now it is straightforward to see that the resulting admissible graph is the regular multigraph of Fig. 1 (right).

4.4 Relation among admissible graphs

The central questions raised about the realization of admissible graphs of Section 4.1 regard the number of possible graphs as well as the relation among them, with respect to isomorphism and ODE-equivalence. Here we present the results providing the answers.

We start with an example of two non-isomorphic but ODE-equivalent admissible graphs. These are the 4-cell network graphs of Subsection 4.2 obtained in step 4 of the procedure. Let

\mathcal{G}_4^1 be the graph of Fig. 5 on the left. Its adjacency matrices are

$$A_{\mathcal{G}_4^1}^{\rightarrow} = \begin{bmatrix} 0 & 0 & 1 & 1 \\ 1 & 0 & 1 & 1 \\ 1 & 1 & 0 & 0 \\ 1 & 1 & 1 & 0 \end{bmatrix}, \quad A_{\mathcal{G}_4^1}^{\leftarrow} = \begin{bmatrix} 0 & 1 & 0 & 0 \\ 0 & 0 & 0 & 0 \\ 0 & 0 & 0 & 1 \\ 0 & 0 & 0 & 0 \end{bmatrix}.$$

Hence,

$$\mathcal{L}(\mathcal{G}_4^1; \mathbb{R}^n) = \left\{ \begin{bmatrix} t & t^{\leftarrow} & t^{\rightarrow} & t^{\rightarrow} \\ s^{\rightarrow} & s & s^{\rightarrow} & s^{\rightarrow} \\ t^{\rightarrow} & t^{\rightarrow} & t & t^{\leftarrow} \\ s^{\rightarrow} & s^{\rightarrow} & s^{\rightarrow} & s \end{bmatrix} : t, s, t^{\rightarrow}, s^{\rightarrow}, t^{\leftarrow} \in \mathbb{R} \right\}.$$

Now let \mathcal{G}_4^2 be the other graph in Fig. 5 (right). Its adjacency matrices are

$$A_{\mathcal{G}_4^2}^{\rightarrow} = \begin{bmatrix} 0 & 0 & 1 & 1 \\ 0 & 0 & 0 & 0 \\ 1 & 1 & 0 & 0 \\ 0 & 0 & 0 & 0 \end{bmatrix}, \quad A_{\mathcal{G}_4^2}^{\leftarrow} = \begin{bmatrix} 0 & 1 & 0 & 0 \\ 1 & 0 & 1 & 1 \\ 0 & 0 & 0 & 1 \\ 1 & 1 & 1 & 0 \end{bmatrix}.$$

Hence,

$$\mathcal{L}(\mathcal{G}_4^2; \mathbb{R}^n) = \left\{ \begin{bmatrix} t & t^{\leftarrow} & t^{\rightarrow} & t^{\rightarrow} \\ s^{\leftarrow} & s & s^{\leftarrow} & s^{\leftarrow} \\ t^{\rightarrow} & t^{\rightarrow} & t & t^{\leftarrow} \\ s^{\leftarrow} & s^{\leftarrow} & s^{\leftarrow} & s \end{bmatrix} : t, s, t^{\rightarrow}, t^{\leftarrow}, s^{\leftarrow} \in \mathbb{R} \right\}.$$

Therefore,

$$\mathcal{L}(\mathcal{G}_4^1; \mathbb{R}^n) = \mathcal{L}(\mathcal{G}_4^2; \mathbb{R}^n),$$

so \mathcal{G}_4^1 and \mathcal{G}_4^2 are ODE-equivalent. But they are clearly non isomorphic.

As we have already seen, step 4 refines the relations of step 3, when the quantity of admissible graphs is attained:

Proposition 4.2. *The number of possible distinct equivalence relations \sim_3 (step 3) is given by*

$$\vartheta(f) = \prod_{Q \in \mathcal{C}/\sim_1} \left(\prod_{t=1}^v (u_t!)^{(|Q|-1)} \right). \quad (4.13)$$

Proof. We use the notation of Remark 4.1 (b). For each I -class Q , we have u_1, \dots, u_v uniquely determined. Based on the possible partitions of (4.8) which satisfy (4.9), it follows that, for each $c \in Q$, we have v collections of edge sets (4.7) such that the sets in each collection can be permuted in \hat{f}_c . Hence, once we choose $c = c_0 \in Q$ as a reference, for each $d \in Q - \{c_0\}$ the equation (4.5) has

$$\prod_{t=1}^v u_t!$$

ways to be satisfied. □

From a fixed choice of the associated generating functions, the next three results specify how the resulting admissible graphs are related.

Theorem 4.3. *For a given C^1 vector field, the realization procedure of Subsection 4.1 yields admissible graphs with the following relations:*

- (1) *The network graph $\mathcal{G}_1 = (\mathcal{C}, \mathcal{E}, \sim_{\mathcal{C}}, \sim_1)$ of step 1 and the network graphs $\mathcal{G}_2 = (\mathcal{C}, \mathcal{E}, \sim_{\mathcal{C}}, \sim_2)$ of step 2 are unique up to an isomorphism;*
- (2) *Each $\mathcal{G}_4 = (\mathcal{C}, \mathcal{E}, \sim_{\mathcal{C}}, \sim_4)$ of step 4 may be non isomorphic to another network graph obtained in this step, but it is ODE-equivalent to some \mathcal{G}_3 of step 3;*
- (3) *The following inclusions hold:*

$$\mathcal{L}(\mathcal{G}_4; \mathbb{R}^{n_0}) = \mathcal{L}(\mathcal{G}_3; \mathbb{R}^{n_0}) \subseteq \mathcal{L}(\mathcal{G}_2; \mathbb{R}^{n_0}) \subseteq \mathcal{L}(\mathcal{G}_1; \mathbb{R}^{n_0}).$$

Proof. We prove by remarking the four steps of the procedure from the adjacency matrix point of view. For simplicity, the proof is carried out for the construction of simple graphs. For multigraphs the proof is completely analogous adapting the notation of an edge which is not identified with a pair of vertices and so adjacency matrices have integer entries instead of only 0 and 1.

In step 1, for a choice of \mathcal{C} , there is a one-to-one correspondence between the edges in \mathcal{E} and adjacency matrices: each adjacency matrix $A_1^{i,j}$ corresponds to $(i, j) \in \mathcal{E}$, with the ji -entry equal to 1 and the others equal to zero. Such matrices are unique up to vertex labeling.

In step 2, for each $c \in \mathcal{C}$ consider the partition (4.4) of $I(c)$. The adjacency matrices are, for each $r' = 1, \dots, r$,

$$A_2^{c,r'} = \sum_{d \in K_{r'}} A_1^{d,c},$$

so that the graph is unique up to an isomorphism.

In step 3, we construct the I -classes of cells. For each I -class Q , the adjacency matrices are

$$A_3^{Q,r'} = \sum_{c \in Q} A_2^{c,r'} \quad r' = 1, \dots, r.$$

As already registered in Remark 4.1 (b), such matrices depend on the ordination of variables in each component; in addition, $\vartheta(f)$ is the number of all possible ordinations, by Proposition 4.2; so distinct choices may lead to isomorphic graphs.

At this point, it is already straightforward to see that the two inclusions in item (3) hold. So we finally prove the statement in (2).

Without loss of generality, assume that the graph \mathcal{G}_3 has two I -classes $R = \{1, \dots, m\}$, $S = \{m+1, \dots, n_0\}$. Since $R \cap S = \emptyset$, then the null rows of $A_3^{R,r'}$ are non null rows in $A_3^{S,s'}$, and vice

versa. The adjacency matrices of a graph \mathcal{G}_4 in step 4 are as follows:

$$\begin{aligned} A_3^{R,r''} & , \quad r'' = 1, \dots, r \text{ and } r'' \neq r', \\ A_3^{S,s''} & , \quad s'' = 1, \dots, s \text{ and } s'' \neq s', \\ B_4 = A_3^{R,r'} + A_3^{S,s'} & . \end{aligned}$$

Thus, $M \in \mathcal{L}(\mathcal{G}_4, \mathbb{R}^{n_0})$ if, and only if,

$$\begin{aligned} M & = \text{diag}(\overbrace{t, \dots, t}^{m \text{ times}}, \overbrace{\bar{t}, \dots, \bar{t}}^{n_0 - m \text{ times}}) + \sum_{r'' \neq r'} \text{diag}(t^{r''}, \dots, t^{r''}, 0, \dots, 0) A_3^{R,r''} + \\ & + \sum_{s'' \neq s'} \text{diag}(0, \dots, 0, t^{s''}, \dots, t^{s''}) A_3^{S,s''} \\ & + \text{diag}(t^{r'}, \dots, t^{r'}, t^{s'}, \dots, t^{s'}) (A_3^{R,r''} + A_3^{S,s''}) \\ & = \text{diag}(t, \dots, t, \bar{t}, \dots, \bar{t}) + \sum_{r''} \text{diag}(t^{r''}, \dots, t^{r''}, 0, \dots, 0) A_3^{R,r''} + \\ & + \sum_{s''} \text{diag}(0, \dots, 0, t^{s''}, \dots, t^{s''}) A_3^{S,s''}, \end{aligned} \quad (4.14)$$

which is a general element of $\mathcal{L}(\mathcal{G}_3; \mathbb{R}^{n_0})$. Therefore, $\mathcal{L}(\mathcal{G}_4; \mathbb{R}^{n_0}) = \mathcal{L}(\mathcal{G}_3; \mathbb{R}^{n_0})$. This equality holds for any choice of the pair of indices r', s' as long as the I -classes are kept unchanged, so this concludes the proof. \square

In the remaining of this section we discuss how the $\vartheta(f)$ graphs of step 3 are related according to the ODE-equivalence. We assume that the vector field is smooth and that the cells of the resulting network graphs with, say, n cells, have the same dimension.

Without loss of generality, we assume that each cell phase space is one-dimensional. To ease the exposition, we present the details for the simplest but sufficiently general case: For a smooth vector field $f: \mathbb{R}^n \rightarrow \mathbb{R}^n$, suppose that step 3 results in two input classes $\{1, \dots, n_0\}$ and $\{n_0 + 1, \dots, n\}$ with associated generating functions g and h ,

$$\begin{aligned} g(y, \overline{y_1, \dots, y_k}, \overline{y_{k+1}, \dots, y_{2k}}, \overline{y_{2k+1}, \dots, y_l}) & = g(y, \overline{y_{k+1}, \dots, y_{2k}}, \overline{y_1, \dots, y_k}, \overline{y_{2k+1}, \dots, y_l}) \\ h(y, \overline{y_1, \dots, y_{k'}}, \overline{y_{k'+1}, \dots, y_{2k'}}) & = h(y, \overline{y_{k'+1}, \dots, y_{2k'}}, \overline{y_1, \dots, y_{k'}}). \end{aligned} \quad (4.15)$$

We have $\vartheta(f) = 2^{n_0-1} 2^{n-n_0-1} = 2^{n-2}$ graphs, and let \mathcal{G} be one of the graphs. Then \mathcal{G} has five adjacency matrices $A_{\mathcal{G}}^i$, $i = 1, \dots, 5$, three of which (say for $i = 1, 2, 3$) having the last $n - n_0$ null rows and two ($i = 4, 5$) having the first n_0 null rows.

We now give a technical definition.

Definition 4.4. *With the notation of Remark 4.1(b), let \mathcal{G} be a network graph determined by the partition (4.8). The network graph $\tilde{\mathcal{G}}$ is given by defining its \mathcal{E} -classes as the unions*

$$K^1 \cup \dots \cup K^{u_1}, K^{u_1+1} \cup \dots \cup K^{u_1+u_2}, \dots, K^{u_1+\dots+u_{v-1}+1} \cup \dots \cup K^{u_1+\dots+u_v},$$

for each I -class Q and each $c \in Q$.

For the case (4.15), $\bar{\mathcal{G}}$ is the graph whose adjacency matrices are

$$A_{\mathcal{G}}^1 + A_{\mathcal{G}}^2, A_{\mathcal{G}}^3, A_{\mathcal{G}}^4 + A_{\mathcal{G}}^5.$$

Remark 4.5. The graph $\bar{\mathcal{G}}$ does not depend on the particular choice of \mathcal{G} , but only on the associated generating functions.

Let $\gamma: \mathcal{C} \rightarrow \mathcal{C}$ be a bijection that preserves the input classes of \mathcal{G} . The graph $\gamma\mathcal{G}$, whose adjacency matrices are $\gamma A_{\mathcal{G}}^i \gamma^{-1}$, for $i = 1, \dots, 5$, is ODE-equivalent to \mathcal{G} . However, it is not necessarily true that $\gamma\mathcal{G}$ is also an admissible graph for this vector field. So under what conditions over γ is this an admissible graph? The following proposition gives a necessary condition:

Proposition 4.6. *For generic generating functions and for \mathcal{G} an admissible graph, if $\gamma\mathcal{G}$ is an admissible graph, then there exists $\gamma' = (\gamma_{\mathcal{C}}, \gamma_{\mathcal{E}}) \in \text{Aut}(\bar{\mathcal{G}})$ such that $\gamma = \gamma_{\mathcal{C}}$.*

Proof. To ease exposition, we present the proof for the case in (4.15). For any $a \in \mathbb{R}$, we take $\mathbf{v} = (a, \dots, a) \in \mathbb{R}^n$. Let us also denote by \mathbf{v} the vectors in \mathbb{R}^{l+1} and $\mathbb{R}^{2k'+1}$ with all entries equal to a . By the permutation symmetries of g, h , we have that

$$\frac{\partial g}{\partial y_1}(\mathbf{v}) = \frac{\partial g}{\partial y_{k+1}}(\mathbf{v}), \quad \frac{\partial h}{\partial y_1}(\mathbf{v}) = \frac{\partial h}{\partial y_{k'+1}}(\mathbf{v}).$$

Since f is \mathcal{G} -admissible, these imply that

$$Df(\mathbf{v}) = \alpha + \frac{\partial g}{\partial y_1}(\mathbf{v})(A_{\mathcal{G}}^1 + A_{\mathcal{G}}^2) + \frac{\partial g}{\partial y_{2k+1}}(\mathbf{v})A_{\mathcal{G}}^3 + \frac{\partial h}{\partial y_1}(\mathbf{v})(A_{\mathcal{G}}^4 + A_{\mathcal{G}}^5),$$

where α is a diagonal matrix whose first n_0 entries are equal to $\frac{\partial g}{\partial y_1}(\mathbf{v})$ and the last $n - n_0$ entries are equal to $\frac{\partial h}{\partial y_1}(\mathbf{v})$. Similarly, as f is $\gamma\mathcal{G}$ -admissible, then

$$Df(\mathbf{v}) = \alpha + \frac{\partial g}{\partial y_1}(\mathbf{v})\gamma(A_{\mathcal{G}}^1 + A_{\mathcal{G}}^2)\gamma^{-1} + \frac{\partial g}{\partial y_{2k+1}}(\mathbf{v})\gamma A_{\mathcal{G}}^3 \gamma^{-1} + \frac{\partial h}{\partial y_1}(\mathbf{v})\gamma(A_{\mathcal{G}}^4 + A_{\mathcal{G}}^5)\gamma^{-1}.$$

Comparing the null rows, the following equalities hold:

$$\begin{aligned} \frac{\partial g}{\partial y_1}(\mathbf{v})(A_{\mathcal{G}}^1 + A_{\mathcal{G}}^2) + \frac{\partial g}{\partial y_{2k+1}}(\mathbf{v})A_{\mathcal{G}}^3 &= \frac{\partial g}{\partial y_1}(\mathbf{v})\gamma(A_{\mathcal{G}}^1 + A_{\mathcal{G}}^2)\gamma^{-1} + \frac{\partial g}{\partial y_{2k+1}}(\mathbf{v})\gamma A_{\mathcal{G}}^3 \gamma^{-1} \\ \frac{\partial h}{\partial y_1}(\mathbf{v})(A_{\mathcal{G}}^4 + A_{\mathcal{G}}^5) &= \frac{\partial h}{\partial y_1}(\mathbf{v})\gamma(A_{\mathcal{G}}^4 + A_{\mathcal{G}}^5)\gamma^{-1} \end{aligned}$$

If there exist a_1, a_2, a_3 such that

$$\det \begin{bmatrix} \frac{\partial g}{\partial y_1}(\mathbf{v}_1) & \frac{\partial g}{\partial y_{2k+1}}(\mathbf{v}_1) \\ \frac{\partial g}{\partial y_1}(\mathbf{v}_2) & \frac{\partial g}{\partial y_{2k+1}}(\mathbf{v}_2) \end{bmatrix} \neq 0 \quad \text{e} \quad \frac{\partial h}{\partial y_1}(\mathbf{v}_3) \neq 0, \quad (4.16)$$

(this is the generic condition on g, h), then

$$A_{\mathcal{G}}^1 + A_{\mathcal{G}}^2 = \gamma(A_{\mathcal{G}}^1 + A_{\mathcal{G}}^2)\gamma^{-1}, \quad A_{\mathcal{G}}^3 = \gamma A_{\mathcal{G}}^3 \gamma^{-1}, \quad A_{\mathcal{G}}^4 + A_{\mathcal{G}}^5 = \gamma(A_{\mathcal{G}}^4 + A_{\mathcal{G}}^5)\gamma^{-1}.$$

But this means that γ is a bijection on the set of cells of \mathcal{G} by an automorphism of $\bar{\mathcal{G}}$. \square

Theorem 4.7. Let $\gamma' = (\gamma_{\mathcal{E}}, \gamma_{\mathcal{G}}) \in \text{Aut}(\bar{\mathcal{G}})$.

(1) The vector field f is \mathcal{G} -admissible and $\gamma_{\mathcal{E}}\mathcal{G}$ -admissible if, and only if, the bijection $\gamma_{\mathcal{E}}$ induces a bijection on the input sets (step 2) preserving them as partitions, that is,

$$\gamma_{\mathcal{E}}(I(c)) = I(\gamma_{\mathcal{E}}(c)), \text{ as partitions.} \quad (4.17)$$

(2) The condition (4.17) on γ' implies that $f\gamma_{\mathcal{E}} = \gamma_{\mathcal{E}}f$. The converse holds for the simple graph case.

Proof. (1) If (4.17) holds, then it is direct from Definition 2.3 that f is $\gamma_{\mathcal{E}}\mathcal{G}$ -admissible, since $\gamma_{\mathcal{E}}$ preserves input sets. If (4.17) does not hold, then there exists $c \in \mathcal{C}$ such that $\gamma_{\mathcal{E}}(I(c)) \neq I(\gamma_{\mathcal{E}}(c))$; by uniqueness of the partition of $I(\gamma_{\mathcal{E}}(c))$, it follows that f is not $\gamma_{\mathcal{E}}\mathcal{G}$ -admissible.

(2) For $c \in \{1, \dots, n_0\}$, we have that

$$(f\gamma_{\mathcal{E}})_c(x_1, \dots, x_n) = f_c(x_{\gamma_{\mathcal{E}}^{-1}(1)}, \dots, x_{\gamma_{\mathcal{E}}^{-1}(n)}) = g(x_{\gamma_{\mathcal{E}}^{-1}(c)}, x_{\gamma_{\mathcal{E}}^{-1}(I(c))})$$

and

$$(\gamma_{\mathcal{E}}f)_c(x_1, \dots, x_n) = f_{\gamma_{\mathcal{E}}^{-1}(c)}(x_1, \dots, x_n) = g(x_{\gamma_{\mathcal{E}}^{-1}(c)}, x_{I(\gamma_{\mathcal{E}}^{-1}(c))}),$$

so the equality $f\gamma_{\mathcal{E}} = \gamma_{\mathcal{E}}f$ follows from (4.17). For the converse, suppose that $f\gamma_{\mathcal{E}} = \gamma_{\mathcal{E}}f$, so

$$g(x_{\gamma_{\mathcal{E}}^{-1}(c)}, x_{\gamma_{\mathcal{E}}^{-1}(I(c))}) = g(x_{\gamma_{\mathcal{E}}^{-1}(c)}, x_{I(\gamma_{\mathcal{E}}^{-1}(c))}).$$

But (4.17) to fail would contradict the maximality of the parts of $I(\gamma_{\mathcal{E}}^{-1}(c))$ for simple graphs. \square

Corollary 4.8. Let \mathcal{G} be an admissible simple graph of step 3 for f . Any admissible graph for f and nonisomorphic to \mathcal{G} is ODE-equivalent to \mathcal{G} if, and only if, it is of the form $\sigma\mathcal{G}$, where σ belongs to

$$\Sigma(\mathcal{G}) = \{\gamma \in \text{Aut}(\bar{\mathcal{G}}) \mid \gamma f = f\gamma\} / \text{Iso}(\mathcal{G}).$$

Proof. This is direct from Theorem 4.7 (2). \square

The example of the next subsection illustrates that distinct choices of step 3 can lead to isomorphic graphs or also to non ODE-equivalent graphs.

4.5 Example: a vector field on \mathbb{R}^6

The aim of this section is to show with an example that a vector field may admit invariant polydiagonal subspaces that are not realized as a synchrony pattern of an admissible graph of this vector field. Nevertheless, for this particular example of six cells we shall verify that the polydiagonal invariant subspaces are generically realized as synchronies of the network graph $\bar{\mathcal{G}}$ presented above.

We construct admissible simple graphs for vector fields $f : \mathbb{R}^6 \rightarrow \mathbb{R}^6$ that govern systems of the form

$$\begin{aligned} \dot{x}_1 &= g(x_1, x_5, x_6, x_2, x_3) \\ \dot{x}_2 &= g(x_2, x_6, x_1, x_3, x_4) \\ \dot{x}_3 &= g(x_3, x_1, x_2, x_4, x_5) \\ \dot{x}_4 &= g(x_4, x_2, x_3, x_5, x_6) \\ \dot{x}_5 &= g(x_5, x_3, x_4, x_6, x_1) \\ \dot{x}_6 &= g(x_6, x_4, x_5, x_1, x_2), \end{aligned} \tag{4.18}$$

for $g : \mathbb{R}^5 \rightarrow \mathbb{R}$ such that

$$g(y, \overline{y_1, y_2, y_3, y_4}) = g(y, \overline{y_3, y_4, y_1, y_2}). \tag{4.19}$$

Notice that \mathcal{G} in this case is the graph G_6 of six cells with nearest and next nearest neighbor coupling. The synchrony subspaces of G_6 are given in Table 1.

Clearly, an optimized admissible simple graph for f with six cells is homogeneous with two types of edges. From (4.19), there are $\vartheta(f) = 2^{6-1} = 32$ ways to define the edge classes. By investigation, it is easy to see that, up to isomorphism, there are eight types of admissible simple graphs. By Proposition 2.4, these are all non ODE-equivalent. In Table 2 we present the eight types of admissible graphs and, for each type representative \mathcal{G} listed in the first column, we give the possible synchrony subspaces. In addition, in the last column we present the number $|\Sigma(\mathcal{G})|$ of the ODE-equivalence class (see Corollary 4.8). Notice that these numbers sum up to give $\vartheta(f)$.

We finally discuss the data presented in Table 2 with respect to the invariant polydiagonal subspaces under f . On one hand, each number in the second column corresponds to a subspace that is obviously invariant under f , by the admissibility of the graphs. On the other hand, let Θ be a polydiagonal subspace which is invariant under f ,

$$f(\Theta) \subseteq \Theta. \tag{4.20}$$

We prove that generically this is a synchrony subspace for some graph \mathcal{G} in Table 2. Let A^1 and A^2 be the adjacency matrices of \mathcal{G} . Since Θ is polydiagonal, it contains the diagonal. So let $v \in \Theta$ be in the diagonal. By (4.19), we have that $\frac{\partial g}{\partial y_1}(v) = \frac{\partial g}{\partial y_3}(v)$, and then

$$\begin{aligned} Df(v)(\Theta) &= \frac{\partial g}{\partial y}(v)\Theta + \frac{\partial g}{\partial y_1}(v)A^1(\Theta) + \frac{\partial g}{\partial y_3}(v)A^2(\Theta) \\ &= \frac{\partial g}{\partial y}(v)\Theta + \frac{\partial g}{\partial y_1}(v)(A^1 + A^2)(\Theta). \end{aligned}$$

If v satisfies the generic condition $\frac{\partial g}{\partial y_1}(v) \neq 0$, then it follows directly from (4.20) that the inclusion $(A^1 + A^2)(\Theta) \subseteq \Theta$ also holds. We now notice that $A^1 + A^2$ is the adjacency matrix of the network graph G_6 . Therefore, Θ is generically induced by a synchrony pattern of G_6 . Now,

G_6 is not an admissible graph for (4.18), but each of its synchrony patterns (Table 1) falls into the second column of Table 2 for some (maybe more than one) graph up to the action of $\text{Aut}(G_6)$.

For the network of the next section, the admissible graph is G_6 and we also discuss about invariant subspaces. We use a similar approach as above, but with an extra linear algebra property provided for that particular case.

4.6 Coupled network of van der Pol identical oscillators

In this section we present the possible synchronous configurations in a specific network of identical oscillators. In particular, we find the hybrid states of chimera, verifying that spatially separated domains of synchronized and desynchronized behavior can arise in networks of identical units with symmetric coupling topologies.

We consider a network of six second-order systems of van der Pol type identical oscillators which are coupled in a non-local fashion with additional intensity-dependent frequency (CHANDRASEKAR *et al.*, 2014):

$$\ddot{x}_i = b(1 - x_i^2)\dot{x}_i - (\omega_0^2 + \alpha_1 x_i^2 + \alpha_2 x_i^4)x_i + \varepsilon \left(\frac{1}{4} \left(\sum_{j=i-2}^{j=i+2} \dot{x}_j \right) - \dot{x}_i \right) + \eta \left(\frac{1}{4} \left(\sum_{j=i-2}^{j=i+2} x_j \right) - x_i \right), \quad (4.21)$$

for $i = 1, \dots, 6$, where α_1 and α_2 are the so-called intensity parameters, ε and η are the coupling strengths.

A network of several systems of van der Pol type identical oscillators was numerically studied in (CHANDRASEKAR *et al.*, 2014) for 500 oscillators. That work shows that from a random initial condition the system can evolve to a situation where part of the oscillators are in synchrony and the other part are in total incoherence of phases.

In 1665, Christiaan Huygens observed that two pendulum clocks always synchronized after a certain time. The justification was that, for being stuck in the same wood, part of the momentum of one pendulum traveled as vibrations in the wood to the other pendulum. Since then, it was thought that a set of coupled oscillators either remained in total disorder or, after a certain time, got in synchrony. However, as first observed by Kuramoto and Battogtokh (KURAMOTO; BATTOGTOKH, 2002), for the coupling of identical oscillators there can be an intermediate state between total synchrony (coherence) and total desynchrony (incoherence). In this regime, part of the oscillators are synchronized and the other part are in total incoherence of phases. This phenomenon, known as ‘chimera state’ after Abrams and Strogatz (ABRAMS; STROGATZ, 2006), has since attracted attention and enormous interest in many fields of applications. Experiments and numerical simulations have given evidences that this behaviour is not only possible but also expected to be stable as the system evolves.

We investigate synchronous states of (4.21), namely

$$x_i(t) = x_j(t), \forall t \in \mathbb{R}, \quad (4.22)$$

for i, j in some subset of $\{1, \dots, 6\}$.

Notice that, in particular, $\dot{x}_i(t) = \dot{x}_j(t)$. Hence, if we rewrite (4.21) as the coupled Hamiltonian system

$$\begin{aligned} \dot{x}_i &= y_i \\ \dot{y}_i &= b(1 - x_i^2)y_i - (\omega_0^2 + \alpha_1 x_i^2 + \alpha_2 x_i^4)x_i \\ &\quad + \varepsilon \left(\frac{1}{4} \sum_{j=i-2}^{j=i+2} y_j \right) - y_i + \eta \left(\frac{1}{4} \sum_{j=i-2}^{j=i+2} x_j \right) - x_i, \end{aligned} \quad (4.23)$$

for $i = 1, \dots, 6$, then the synchronies of one are in one-to-one correspondence with the synchronies of the other.

This is a vector field admissible for the regular network graph G_6 with six cells on $(\mathbb{R}^2)^6$ with nearest and next nearest neighbor identical coupling. Including the trivial totally synchronous pattern, there are nine distinct patterns of synchrony, which have been computed from our code (see Remark 3.2 and Appendix A). In Table 1 we present all the possible eight nontrivial synchronies. In this particular case, each synchrony subspace is the fixed-point subspace of a subgroup of the automorphism group $\text{Aut}(G_6)$ of the network graph, which is the octahedral group $\mathbf{O} \simeq \langle \mathbf{D}_6, (14), (25) \rangle$ (see (GOLUBITSKY; NICOL; STEWART, 2004, Lemma 2.1), where the authors present the automorphism groups $\text{Aut}(G_N)$, $N \geq 5$).

Regarding the data of Table 1, contrarily to what is usual in the literature, we give all the possible algebraic expressions (second column) of the corresponding diagram (first column), which are obviously fixed-point subspaces of conjugate isotropies. Doing so, we link the data of Tables 1 and 2: expressions (1) to (3) of #1 in Table 1 appear in Table 2 #6 but not in #2; similarly, the expressions (19) to (22) of #6 in Table 1 appear in #6 but only (21) appear in #6 of Table 2, and so on.

Chimera states can now be selected directly from Table 1, namely configurations #1 to #4. For example, in case #2 the cells 3 and 6 are two isolated desynchronized cells. From the point of view of the applications, the detection of the possible robust attracting chimeras from this list is a relevant issue, for these correspond to the numerically observed phenomena of the literature mentioned in our introductory section. At the present, this investigation has been carried out.

By the condition in (3.2), all synchrony subspaces are polydiagonal invariant subspaces under the vector field f defined by (4.23). We finish by investigating the converse. Let Θ be a polydiagonal subspace which is invariant under the vector field f given in (4.23).

In particular, it is invariant under the linearization at the origin,

$$Df(0) = I_6 \otimes \begin{bmatrix} 0 & 1 \\ -\omega_0^2 - \frac{3\eta}{4} & b - \frac{3\varepsilon}{4} \end{bmatrix} + A_{G_6} \otimes \begin{bmatrix} 0 & 0 \\ \frac{\eta}{4} & \frac{\varepsilon}{4} \end{bmatrix},$$

which implies that $A_{G_6} \otimes \begin{bmatrix} 0 & 0 \\ \frac{\eta}{4} & \frac{\varepsilon}{4} \end{bmatrix} [\Theta] \subset \Theta$. Now, since any vector $v \in \Theta$ is of the form $v = (x_1, y_1, \dots, x_6, y_6)$ with $x_i = x_j$ and $y_i = y_j$ for i, j in some subset of $\{1, \dots, 6\}$, and that

$$A_{G_6} \otimes \begin{bmatrix} 0 & 0 \\ \frac{\eta}{4} & \frac{\varepsilon}{4} \end{bmatrix} [v] = \frac{1}{4} A_{G_6} \otimes I_2 [(0, \eta x_1 + \varepsilon y_1, \dots, 0, \eta x_6 + \varepsilon y_6)] \in \Theta,$$

it follows that Θ' is an A_{G_6} -invariant subspace of \mathbb{R}^6 , in the x_i 's variables, defined by the same equalities as for Θ .

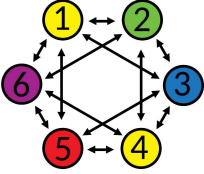
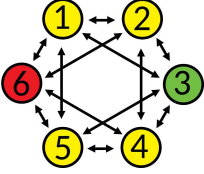
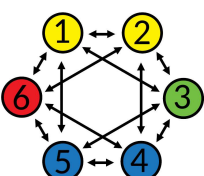
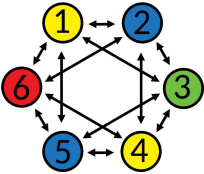
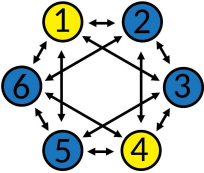
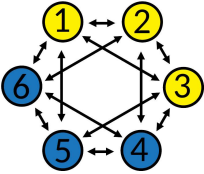
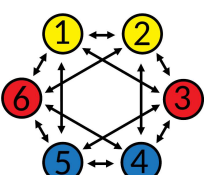
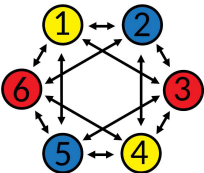
#	Diagram	Algebraic expression	Symmetry of the pattern under the standard representation of the octahedral group
1		(1) $\{x_1 = x_4\}$ (2) $\{x_2 = x_5\}$ (3) $\{x_3 = x_6\}$	Reflection w.r.t. the plane through the other four cells.
2		(4) $\{x_1 = x_2 = x_4 = x_5\}$ (5) $\{x_1 = x_3 = x_4 = x_6\}$ (6) $\{x_2 = x_3 = x_5 = x_6\}$	Rotation of $\pi/2$ w.r.t. an axis through opposite cells.
3		(7) $\{x_1 = x_2, x_4 = x_5\}$ (8) $\{x_1 = x_3, x_4 = x_6\}$ (9) $\{x_1 = x_5, x_2 = x_4\}$ (10) $\{x_1 = x_6, x_3 = x_4\}$ (11) $\{x_2 = x_3, x_5 = x_6\}$ (12) $\{x_2 = x_6, x_3 = x_5\}$	Reflection to the plane through opposite cells and opposite edges.
4		(13) $\{x_1 = x_4, x_2 = x_5\}$ (14) $\{x_1 = x_4, x_3 = x_6\}$ (15) $\{x_2 = x_5, x_3 = x_6\}$	Rotation of π of the octahedron w.r.t the line through opposite cells.
5		(16) $\{x_1 = x_2 = x_4 = x_5, x_3 = x_6\}$ (17) $\{x_1 = x_3 = x_4 = x_6, x_2 = x_5\}$ (18) $\{x_1 = x_4, x_2 = x_3 = x_5 = x_6\}$	Rotation of $\pi/2$ w.r.t. an axis through opposite cells and a reflection w.r.t. the perpendicular plane.
6		(19) $\{x_1 = x_2 = x_3, x_4 = x_5 = x_6\}$ (20) $\{x_1 = x_2 = x_6, x_3 = x_4 = x_5\}$ (21) $\{x_1 = x_3 = x_5, x_2 = x_4 = x_6\}$ (22) $\{x_1 = x_5 = x_6, x_2 = x_3 = x_4\}$	Rotation of $2\pi/3$ w.r.t. the line that cuts the opposite faces.
7		(23) $\{x_1 = x_2, x_3 = x_6, x_4 = x_5\}$ (24) $\{x_1 = x_3, x_2 = x_5, x_4 = x_6\}$ (25) $\{x_1 = x_4, x_2 = x_3, x_5 = x_6\}$ (26) $\{x_1 = x_4, x_2 = x_6, x_3 = x_5\}$ (27) $\{x_1 = x_5, x_2 = x_4, x_3 = x_6\}$ (28) $\{x_1 = x_6, x_2 = x_5, x_3 = x_4\}$	Reflection w.r.t. two planes, one through two opposite cells and the other orthogonally through four cells.
8		(29) $\{x_1 = x_4, x_2 = x_5, x_3 = x_6\}$	Rotation of π w.r.t. an axis through opposite cells and a reflection w.r.t. the perpendicular plane.

Table 1 – Synchrony patterns of the network graph G_6 together with their symmetries.

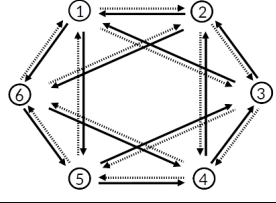
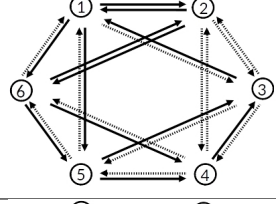
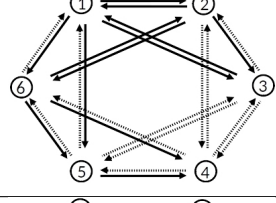
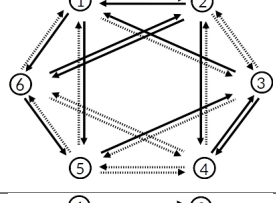
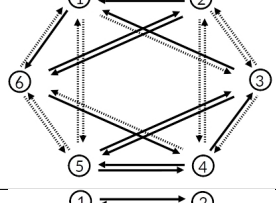
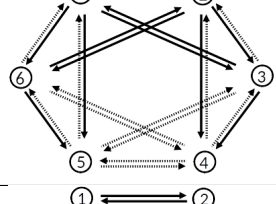
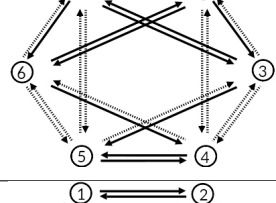
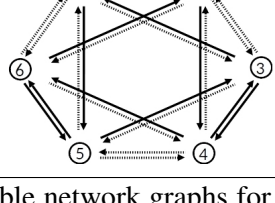
#	\mathcal{G}	Synchrony patterns (numbering extracted from Table 1)	$ \Sigma(\mathcal{G}) $
1		16, 17, 18, 21, 29	1
2		2, 16, 17, 18, 21, 29	6
3		2, 3, 6, 12, 15, 16, 17, 18, 21, 26, 29	6
4		1, 2, 13, 16, 17, 18, 21, 29	6
5		9, 12, 16, 17, 18, 21, 26, 27, 29	3
6		1, 2, 3, 5, 6, 8, 12, 13, 14, 15, 16, 17, 18, 21, 23, 24, 26, 29	3
7		3, 9, 16, 17, 18, 21, 27, 29	6
8		1, 2, 3, 13, 14, 15, 16, 17, 18, 21, 23, 25, 28, 29	1

Table 2 – Admissible network graphs for (4.18) up to ODE-equivalence with their corresponding synchrony patterns. The last column gives the number of admissible graphs nonisomorphic and ODE-equivalent to the graph.

SYNCHRONY PATTERNS IN LAPLACIAN NETWORKS

This chapter is devoted to the class of networks whose admissible maps are attached to the associated graph not only through its architecture but also through the Laplacian matrix of the graph. As mentioned in the Introduction, these generalize the traditional Kuramoto model.

In Section 5.1 we recall the graph Laplacian matrix and present a result from algebraic graph theory for Laplacian matrices. Section 5.2 is dedicated to present the general algebraic expression of an admissible map of a Laplacian network. Finally, the extra admissible additive structure behind the Kuramoto networks is dealt with in Section 5.3. The results in this Chapter appear in (AMORIM; MANOEL, 2023)

5.1 Graph Laplacian matrix

For a bidirected graph G with n vertices, recall that the Laplacian matrix is

$$L = D - A,$$

where D is the diagonal matrix of the valencies of the vertices and A is the adjacency matrix. The ii -entry of D is the degree of the vertex i if G is unweighted, and $\sum_{j=1}^n w_{ij}$ if G is a weighted graph. A is, as usual, the sum of the adjacency matrices (2.1) for unweighted edge classes and considering weights w_{ij} instead of 1's for weighted graphs.

It is direct from the definition that 0 is an eigenvalue of L with eigenvector $(1, \dots, 1)$. For weighted connected graphs with possibly negative weights, the authors in (BRONSKI; DEVILLE, 2014, Theorem 2.10) give the best possible bounds on the numbers of positive, negative and zero eigenvalues. The next result generalizes their result for disconnected graph, which is used in the next sections.

Let G_+ (resp. G_-) denote the subgraph with the same vertex set as G together with the edges of positive (resp. negative) weights. Let n_0, n_- and n_+ denote the numbers of zero, negative and positive eigenvalues of the Laplacian L , and let $c(G)$ denote the number of connected components of G .

Theorem 5.1. *If G is a (possibly disconnected) graph, then*

$$\begin{aligned} c(G_+) - c(G) &\leq n_+(L) \leq n - c(G_-) \\ c(G_-) - c(G) &\leq n_-(L) \leq n - c(G_+) \\ c(G) &\leq n_0(L) \leq n + 2c(G) - c(G_+) - c(G_-). \end{aligned} \tag{5.1}$$

Proof. If G has k connected components, for $i = 1, \dots, k$, let G_i denote the connected components with n_i vertices, so $n_1 + \dots + n_k = n$. Reorder the rows and columns of L if necessary to assume that L is a block diagonal matrix

$$L = \text{diag}(L_1, \dots, L_k).$$

By the estimates in (BRONSKI; DEVILLE, 2014), for each $i = 1, \dots, k$ we have $c(\mathcal{G}_{i+}) - 1 \leq n_+(L_i) \leq n_i - c(G_{i-})$, so

$$\begin{aligned} c(G_{1+}) + \dots + c(G_{k+}) - k &\leq n_+(L_1) + \dots + n_+(L_k) \leq \\ &\leq n_1 + \dots + n_k - (c(G_{1-}) + \dots + c(G_{k-})), \end{aligned} \tag{5.2}$$

so the first estimate follows. The other inequalities follow similarly. \square

If the graph G is connected, then $c(G) = 1$ and (5.1) are the bounds given in (BRONSKI; DEVILLE, 2014).

We notice that this result involves only topological information about the graph, namely the connectivity of the graph and the sign information on the edge weights. In particular, it follows that, for a graph with n vertices, the difference between the upper and lower bounds in (5.1) is an integer that can vary between 0 and $n - 1$.

5.2 Laplacian mappings

In this section we use the idea of inserting weights on an unweighted graph G to adapt the algebraic graph theory for weighted graphs to the associated Laplacian network graph \mathcal{G} . Let us explain: for a given unweighted graph G , we associate an admissible coupled system (3.1). For our case of interest, the Jacobian $Jf(x)$ of the governing vector field is, at any point x , a Laplacian matrix. The idea is to look at it as a weighted Laplacian of G , considering G as a weighted graph. Under this approach, we use Theorem 5.1.

We start with three definitions:

Definition 5.2. A matrix $L = (l_{ij})$ of order n is a Laplacian matrix if it is symmetric with $l_{ii} = -\sum_{j \neq i} l_{ij}$, for $i = 1, \dots, n$.

Our interest here is to deduce an algebraic expression of a map $f : P \rightarrow P$ on a real vector space P , so for simplicity we assume $P = \mathbb{R}^n$.

Definition 5.3. A map $f : \mathbb{R}^n \rightarrow \mathbb{R}^n$ of class C^1 is a Laplacian map if its Jacobian $Jf(x)$ at any $x \in \mathbb{R}^n$ is a linear map whose matrix is a Laplacian matrix.

The set of Laplacian maps shall be denoted by $LS(\mathbb{R}^n)$.

It follows from the two definitions above that being bidirected is a necessary assumption in this context. We have:

Definition 5.4. For a bidirected graph, an associated network \mathcal{G} is a Laplacian network if the admissible map is a Laplacian map.

For the main result, we need:

Lemma 5.5. If $h : \mathbb{R}^n \rightarrow \mathbb{R}$ is such that

$$\sum_{i=1}^n \frac{\partial h}{\partial x_i}(x) = 0. \quad (5.3)$$

then

$$h(x_1, \dots, x_n) = \alpha(x_1 - x_n, \dots, x_{n-1} - x_n), \quad (5.4)$$

for some $\alpha : \mathbb{R}^{n-1} \rightarrow \mathbb{R}$.

Proof. Consider the change of coordinates $t_i = x_i - x_n$, $i = 1 \dots, n-1$, $t_n = x_n$. We then have

$$h(x_1, \dots, x_n) = h(t_1 + t_n, \dots, t_{n-1} + t_n, t_n) = \tilde{\alpha}(t_1, \dots, t_n).$$

But

$$\frac{\partial \tilde{\alpha}}{\partial t_n} = \sum_i \frac{\partial h}{\partial x_i} = 0.$$

Hence, $\tilde{\alpha}(t_1, \dots, t_n) = \alpha(t_1, \dots, t_{n-1})$, and the result follows. \square

We now present the characterization of the general form of a Laplacian mapping:

Theorem 5.6. $f = (f_1, \dots, f_n) \in LS(\mathbb{R}^n)$ if, and only if,

$$\begin{aligned} f_i(x_1, \dots, x_n) &= \frac{\partial g}{\partial t_i}(x_1 - x_n, \dots, x_{n-1} - x_n), \quad i = 1, \dots, n-1, \\ f_n &= -f_1 - \dots - f_{n-1} + k. \end{aligned}$$

for some $g \in C^2(\mathbb{R}^{n-1})$ and some constant $k \in \mathbb{R}$.

Proof. From Lemma 5.5, we have

$$f_i(x_1, \dots, x_n) = \alpha_i(x_1 - x_n, \dots, x_{n-1} - x_n), \quad i = 1, \dots, n.$$

The Jacobian $Jf(x)$ is symmetric, so

$$\frac{\partial \alpha_i}{\partial t_j} = \frac{\partial \alpha_j}{\partial t_i}, \quad i, j = 1, \dots, n-1, i \neq j, \quad (5.5)$$

$$\frac{\partial \alpha_n}{\partial t_i} = -\frac{\partial \alpha_i}{\partial t_1} - \dots - \frac{\partial \alpha_i}{\partial t_{n-1}} \quad i = 1, \dots, n-1, \quad (5.6)$$

which imply that

$$\frac{\partial \alpha_n}{\partial t_i} = -\frac{\partial \alpha_1}{\partial t_i} - \dots - \frac{\partial \alpha_{n-1}}{\partial t_i} = \frac{\partial}{\partial t_i}(-\alpha_1 - \dots - \alpha_{n-1}), \quad i = 1, \dots, n-1. \quad (5.7)$$

Hence, $\alpha_n = -\sum_{i=1}^{n-1} \alpha_i + k$, for some constant k .

Finally, given any function $g: \mathbb{R}^{n-1} \rightarrow \mathbb{R}$ of class C^2 , we can take $\alpha_i = \frac{\partial g}{\partial t_i}$, $i = 1, \dots, n-1$. Conversely, any map $\alpha = (\alpha_1, \dots, \alpha_{n-1})$ of class C^1 satisfying (5.5) is a gradient mapping. In fact, just set

$$g(t_1, \dots, t_{n-1}) = \sum_{i=1}^{n-1} \int_0^{t_i} \alpha_i(0, \dots, 0, s, t_{i+1}, \dots, t_{n-1}) ds.$$

□

The example below is a simple illustration of Theorem 5.6.

Example 1. For $n = 3$, consider $g(y, z) = \frac{y^2 z^2}{2}$. The following are the coordinate functions of a Laplacian mapping $f: \mathbb{R}^3 \rightarrow \mathbb{R}^3$:

$$\begin{aligned} f_1(x_1, x_2, x_3) &= (x_1 - x_3)(x_2 - x_3)^2 \\ f_2(x_1, x_2, x_3) &= (x_1 - x_3)^2(x_2 - x_3) \\ f_3(x_1, x_2, x_3) &= -(x_1 - x_3)(x_2 - x_3)^2 - (x_1 - x_3)^2(x_2 - x_3). \end{aligned}$$

The next two corollaries follow straightforwardly:

Corollary 5.7. The following linear isomorphism holds:

$$LS(\mathbb{R}^n) \simeq (C^2(\mathbb{R}^{n-1})/\mathbb{R}) \oplus \mathbb{R}.$$

Corollary 5.8. If $f = (f_1, \dots, f_n) \in LS(\mathbb{R}^n)$, then $\sum_{i=1}^n f_i$ is constant.

We end with the characterization of the Laplacian maps, which is also direct from Theorem 5.6:

Theorem 5.9. $f = (f_1, \dots, f_n) \in LS(\mathbb{R}^n)$ if, and only if, f is a gradient map $f = \nabla \bar{g}$, where $\bar{g}(x_1, \dots, x_n) = g(x_1 - x_n, \dots, x_{n-1} - x_n) + kx_n$.

5.3 Laplacian networks with additive structure

Here we consider Laplacian admissible maps $f \in LS(\mathbb{R}^n)$ with the extra condition that each component f_c of cell c has an additive input structure, namely

$$f_c(x) = \sum_{d \neq c} \phi_{cd}(x_c, x_d). \quad (5.8)$$

This structure provides the simplest way to associate an admissible graph following the formalism from Chapter 4: for such a map, we consider the following coupling rule:

$$(a, b) \sim_{\mathcal{E}} (c, d) \Leftrightarrow \phi_{ba} = \phi_{dc}. \quad (5.9)$$

Indeed, the optimized network graph is not unique if occurs something like Remark 4.13 (b). By simplicity suppose that

$$\begin{aligned} f_c &= \phi(x_c, x_{d_1}) + \phi(x_c, x_{d_2}) + \theta(x_c, x_{d_3}) + \theta(x_c, x_{d_4}) = \\ &= \phi(x_c, x_{d_3}) + \phi(x_c, x_{d_4}) + \theta(x_c, x_{d_1}) + \theta(x_c, x_{d_2}). \end{aligned}$$

So taking the derivative of f_c with respect to x_{d_1} we obtain

$$\frac{\partial \theta}{\partial y}(x, y) = \frac{\partial \phi}{\partial y}(x, y),$$

thus $\theta(x, y) = \phi(x, y) + k(x)$. Then we can replace ϕ by $\bar{\phi} = \phi(x, y) + \frac{k(x)}{2}$ and θ by $\bar{\theta}(x, y) = \theta(x, y) - \frac{k(x)}{2}$. In this case $\bar{\phi} = \bar{\theta}$.

We notice that, by Lemma 5.5,

$$f_n(x_1, \dots, x_n) = \alpha_n(x_1 - x_n, \dots, x_{n-1} - x_n) \quad (5.10)$$

and from (5.8),

$$\frac{\partial^2 \alpha_n}{\partial t_i \partial t_j} = \frac{\partial^2 f_n}{\partial x_i \partial x_j} = 0, \quad i \neq j < n. \quad (5.11)$$

Hence, α_n ‘splits the variables’ x_i and x_j , $i \neq j < n$; more precisely,

$$f_n(x_1, \dots, x_n) = \sum_{d < n} \phi_{nd}(x_n - x_d).$$

By the same reasoning, the same condition holds for other components, and so

$$f_c(x) = \sum_{d \neq c} \phi_{cd}(x_c - x_d), \quad \forall c = 1, \dots, n.$$

Since the graph is bidirected, we have $(a, b) \sim_{\mathcal{E}} (b, a)$, and so $\phi_{ba} = \phi_{ab}$. Furthermore, by the Laplacian condition,

$$\phi'_{ab}(x_a - x_b) = -\frac{\partial f_a}{\partial x_b}(x) = -\frac{\partial f_b}{\partial x_a}(x) = \phi'_{ba}(x_b - x_a).$$

Therefore,

$$\phi'_{ab}(x_a - x_b) = \phi'_{ab}(-(x_a - x_b)),$$

that is, all coupling functions must be odd. We have just proved:

Theorem 5.10. *Let \mathcal{G} be a bidirected graph network. If f is a \mathcal{G} -admissible map, then $f \in LS(\mathbb{R}^n)$ has an additive structure if, and only if, each component of f is of the form*

$$f_c(x) = k_{[c]} + \sum_{d \in I(c)} \phi_{[(c,d)]}(x_d - x_c), \quad (5.12)$$

where $\phi_{[(c,d)]}$ is an odd function that depends only on the $[(c,d)]$ -class of the edge (c,d) and $k_{[c]}$ is a constant that depends only on the I -class $[c]$ of c .

The two theorems above imply the following:

Corollary 5.11. *Let \mathcal{G} be a bidirected graph network. Let f be a \mathcal{G} -admissible map. Then $f \in LS(\mathbb{R}^n)$ has an additive structure if, and only if, f is a gradient mapping $f = -\nabla g$, where*

$$g(x) = \sum_{(c,d) \in \mathcal{E}} \Psi_{[(c,d)]}(x_d - x_c) + \sum_{c \in \mathcal{C}} k_{[c]} x_c,$$

$\Psi_{[(c,d)]}$ is an even function that depends only on the $[(c,d)]$ -class of the edge (c,d) and $k_{[c]}$ is a constant determined by the I -class of c .

The example below illustrates the theorem above. This is a nonhomogeneous network graph with six cells, with two I -classes $\{1, 2, 4, 5\}$ and $\{3, 6\}$, given in Fig. 9.

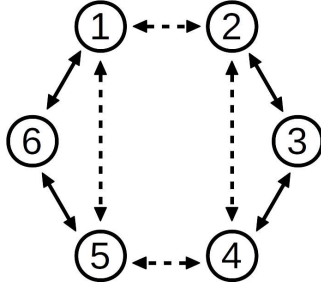


Figure 9 – A nonhomogeneous bidirected graph with six identical cells and two types of edges.

Example 2. *For a bidirected graph with six identical cells and two types of edges as given in Fig. 9, a Laplacian network \mathcal{G} on \mathbb{R}^6 with additive structure is given by*

$$\dot{x} = f(x),$$

where $f = (f_1, \dots, f_6): \mathbb{R}^6 \rightarrow \mathbb{R}^6$,

$$\begin{aligned} f_1(x) &= \kappa + \theta(x_1 - x_2) + \theta(x_1 - x_5) + \phi(x_1 - x_6) \\ f_2(x) &= \kappa + \theta(x_2 - x_1) + \theta(x_2 - x_4) + \phi(x_2 - x_3) \\ f_3(x) &= \ell + \phi(x_3 - x_2) + \phi(x_3 - x_4) \\ f_4(x) &= \kappa + \theta(x_4 - x_2) + \theta(x_4 - x_3) + \phi(x_4 - x_5) \\ f_5(x) &= \kappa + \theta(x_5 - x_1) + \theta(x_5 - x_4) + \phi(x_5 - x_6) \\ f_6(x) &= \ell + \phi(x_6 - x_1) + \phi(x_6 - x_5), \end{aligned}$$

for θ, ϕ any odd functions of class C^1 and κ, ℓ constant.

5.4 Critical points on synchrony subspaces of additive Laplacian networks

The starting point in the study of a dynamical behaviour of a system, or bifurcations with variations of possible external parameters, is the analysis of existence and stability of equilibrium points. Here we proceed in this direction.

In Subsection 5.4.1 we prove that, for any homogeneous additive Laplacian network, Lyapunov stability holds generically for totally synchronous critical points. In the last two subsections we choose two examples to search for critical points with the remaining possible synchrony.

The following result ensures that the investigation of trajectory stability in Laplacian networks is based on the eigenvalues of the Jacobian evaluated at equilibrium points.

Lemma 5.12. *Let $f \in LS(\mathbb{R}^n)$. The α -limit and ω -limit of any trajectory are equilibrium points.*

Proof. From Theorem 5.9, $f \in LS(\mathbb{R}^n)$ is gradient, so the result follows from LaSalle's invariance principle (see for example (WIGGINS, 2003, Section 8.3)). \square

In Subsection 5.4.2 we consider the homogeneous Kuramoto network of six cells with coupling G_6 (identical edges connecting nearest and next nearest neighbors). We list the critical points inside the remaining synchrony subspaces. For each case, we give the estimate for the degree of linear instability through the range of the number of positive eigenvalues. We end with Subsection 5.4.3 doing the same analysis for a homogeneous coupled network of six cells with two types of couplings.

5.4.1 Total synchrony subspace

Let \mathcal{G} be a connected homogeneous bidirected network graph with n cells. Let f be an admissible vector field as in (5.12). We search for critical points, so $k = 0$.

Suppose that there exists $\varepsilon > 0$ such that

$$\alpha \phi_{[(c,d)]}(\alpha) > 0, \forall \alpha \in (-\varepsilon, \varepsilon), \alpha \neq 0. \quad (5.13)$$

Notice that this holds if, in particular, $\phi'_{[(c,d)]}(0) > 0$, for all $(c,d) \in \mathcal{E}$, which can be the case if the primitive of $\phi_{[(c,d)]}$ has a local minimum at zero.

Let Ω be the biggest open hipercilinder around of the total synchrony subspace Δ such that $x \in \Omega$ implies that $|x_d - x_c| < \varepsilon$, for all $(c,d) \in \mathcal{E}$. We then have the following:

Lemma 5.13. (i) Ω is a flow invariant set.

(ii) for $x \in \Omega$, we have $f(x) = 0$ if, and only if, $x \in \Delta$.

Before proving this lemma, we state the following theorem, which is an immediate consequence of this Lemma, since f is gradient (see Corollary 5.11).

Theorem 5.14. *Let \mathcal{G} be a connected homogeneous bidirected network graph. Let f be an admissible vector field as in (5.12) such that (5.13) holds. The total synchrony subspace is asymptotically stable on Ω in the sense of Lyapunov.*

Proof of Lemma 5.13. (i) From Corollary 5.8, $f(x) \cdot (1, \dots, 1) = 0$ for any x . Also, f is constant along the lines parallel to Δ . So it suffices to show that $\Omega \cap \pi$ is flow invariant, where π is the hiperplane $x \cdot (1, \dots, 1) = 0$. To see this, as $\Omega \cap \pi$ is a hipersphere, we just need to show that $f(x) \cdot x < 0$ for all $x \in \Omega \cap \pi \setminus \{0\}$. In fact,

$$\begin{aligned} f(x) \cdot x &= \sum_{c \in \mathcal{C}} \sum_{d \in I(c)} x_c \phi_{[(c,d)]}(x_d - x_c) \\ &= \sum_{(c,d) \in \mathcal{E}} (x_c - x_d) \phi_{[(c,d)]}(x_d - x_c) \leq 0, \end{aligned} \quad (5.14)$$

where at least one portion is strictly less than zero. As \mathcal{G} is connect, (5.14) also shows (ii). \square

We finally mention that if all the functions $\phi_{[(c,d)]}$ are periodic with a comum period, we can restrict the analysis of critical points on the n -torus.

5.4.2 Kuramoto network with G_6 coupling

We consider the Kuramoto network system with six cells and coupling G_6 (Fig. 10):

$$\dot{x}_i = \sum_{j=-2}^2 \sin(x_{i-j} - x_i), \quad i = 1, \dots, 6. \quad (5.15)$$

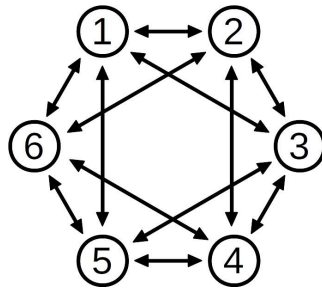


Figure 10 – G_6

We search for the critical points inside synchrony subspaces. It follows from Proposition 3.6 that these are all fixed-point subspaces of subgroups of the automorphism group $Aut(G_6)$, which is the octahedral group. We consider the representation given by permutations,

$$Aut(G_6) = \langle \mathbb{D}_6, (14), (25) \rangle$$

(see (ANTONELI; STEWART, 2006, Lemma 2.1)).

The computation has been carried out starting with the smallest subgroups Σ of $Aut(G_6)$ up to conjugacy, for these will have the largest fixed-point subspaces; and we then continue refining from there. More precisely, we consider the diagram (5.16) with the lattice of fixed-point subspaces, where the arrows represent the refinement by inclusion. The total synchrony has been omitted in this diagram and, apart from it, this is the complete lattice up to conjugacy. Based on this diagram, we start by considering the subgroups Σ such that $Fix(\Sigma)$ correspond to patterns 1 and 3.

$$\begin{array}{ccccc}
 & \text{Pattern 8} & & \text{Pattern 4} & & \text{Pattern 1} \\
 & \text{Fix}\langle(14)(25)(36)\rangle & \longrightarrow & \text{Fix}\langle(14)(25)\rangle & \longrightarrow & \text{Fix}\langle(14)\rangle \\
 & \uparrow & & \uparrow & \nearrow & \\
 & \text{Pattern 5} & & \text{Pattern 2} & & \\
 & \text{Fix}\langle(1245)(36)\rangle & \longrightarrow & \text{Fix}\langle(1245)\rangle & & \\
 & \downarrow & & \downarrow & & \\
 & \text{Pattern 7} & & \text{Pattern 3} & & \\
 & \text{Fix}\langle(12)(36)(45)\rangle & \longrightarrow & \text{Fix}\langle(12)(45)\rangle & & \\
 & & \nearrow & & & \\
 & \text{Pattern 6} & & & & \\
 & \text{Fix}\langle(123)(456)\rangle & & & &
 \end{array} \tag{5.16}$$

Without loss of generality, for all cases we assume that a critical point $x = (x_1, \dots, x_6)$ satisfies $x_1 = 0$.

For $\Sigma = \langle(14)\rangle$, we search for critical points of the form $(0, a, b, 0, c, d)$ for $a, b, c, d \in \mathbb{R} \bmod 2\pi$:

$$\begin{aligned}
 2 \sin(-a) + \sin(b - a) + \sin(d - a) &= 0 \\
 2 \sin(-b) + \sin(a - b) + \sin(c - b) &= 0 \\
 2 \sin(-c) + \sin(b - c) + \sin(d - c) &= 0 \\
 2 \sin(-d) + \sin(a - d) + \sin(c - d) &= 0,
 \end{aligned}$$

which can be rewritten as

$$2 \begin{bmatrix} \sin a \\ \sin c \end{bmatrix} = (\sin b + \sin d) \begin{bmatrix} \cos a \\ \cos c \end{bmatrix} - (\cos b + \cos d) \begin{bmatrix} \sin a \\ \sin c \end{bmatrix} \tag{5.17}$$

$$2 \begin{bmatrix} \sin b \\ \sin d \end{bmatrix} = (\sin a + \sin c) \begin{bmatrix} \cos b \\ \cos d \end{bmatrix} - (\cos a + \cos c) \begin{bmatrix} \sin b \\ \sin d \end{bmatrix} \tag{5.18}$$

Case 1: If $(\sin a, \sin c), (\cos a, \cos c)$ are linearly independent, then (5.17) implies that $\cos b + \cos d = -2$, and so $b = d = \pi$. Using that in (5.18), we get $\sin a = -\sin c$, and so $c = -a$ or

$a = c + \pi$. These give the following two families of critical points:

$$(0, a, \pi, 0, -a, \pi), \quad (0, a, \pi, 0, a + \pi, \pi).$$

If $(\sin b, \sin d), (\cos b, \cos d)$ are linearly independent, then analogously we get the other two families

$$(0, \pi, b, 0, \pi, -b), \quad (0, \pi, b, 0, \pi, b + \pi).$$

Case 2: If both pairs of the previous case are linearly dependent, then each pair form a matrix with zero determinant, and so $\sin(c - a) = 0$ and $\sin(d - b) = 0$. Hence, $c = a$ or $c = a + \pi$ and $b = d$ or $b = d + \pi$.

- If $c = a$ and $d = b$, then $\sin a = \sin(b - a)$ and $\sin b = \sin(a - b)$. So the critical points are

$$(0, \pi, 0, 0, \pi, 0), \quad (0, \frac{4\pi}{3}, \frac{2\pi}{3}, 0, \frac{4\pi}{3}, \frac{2\pi}{3}, 0).$$

- If $c = a$ and $d = b + \pi$, then the critical points are

$$(0, 0, \pi, 0, 0, 0), \quad (0, \pi, b, 0, \pi, b + \pi).$$

For $\Sigma = \langle (12)(45) \rangle$, we search for critical points of the form $(0, 0, a, b, b, c)$, for $a, b, c \in \mathbb{R} \pmod{2\pi}$:

$$\begin{aligned} 2 \sin(-a) + 2 \sin(b - a) &= 0 \\ \sin(-b) + \sin(a - b) + \sin(c - b) &= 0 \\ 2 \sin(-c) + 2 \sin(b - c) &= 0. \end{aligned}$$

These give the following two families of critical points:

$$(0, 0, a, \pi, \pi, -a), \quad (0, 0, a, \pi, \pi, a + \pi).$$

In Table 1 we listed the eight patterns of synchrony of G_6 that are distinct from the total synchrony pattern. Here we follow that order to present in Table 1 the compilation of all (families of) equilibrium points inside the corresponding synchrony pattern.

We then apply Theorem 5.1 to the Jacobian matrix $Jf(x)$, at every critical point x , thought of as a weighted Laplacian of the graph. We refer to the beginning of Subsection 5.2 for the explanation.

For the critical point $x = (0, 0, \pi/2, \pi, \pi, 3\pi/2)$, the Jacobian is

$$Jf(x) = \begin{pmatrix} 0 & +1 & 0 & 0 & -1 & 0 \\ +1 & 0 & 0 & -1 & 0 & 0 \\ 0 & 0 & 0 & 0 & 0 & 0 \\ 0 & -1 & 0 & 0 & +1 & 0 \\ -1 & 0 & 0 & +1 & 0 & 0 \\ 0 & 0 & 0 & 0 & 0 & 0 \end{pmatrix}.$$

Thought of as a graph Laplacian, the graph is as given in Fig. 11. We then have $c(G) = 3$, $c(G_+) = 4$, $c(G_-) = 4$, which gives $1 \leq n_+ \leq 2$. This is one of the possible cases of pattern number 3 of Table 1.

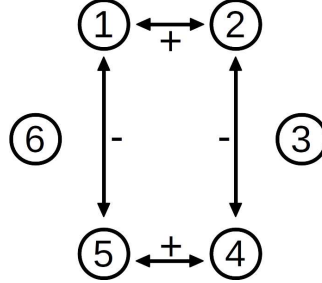


Figure 11 – The disconnected graph obtained from G_6 by assigning $Jf(x)$ as the weighted Laplacian, for $x = (0, 0, \pi/2, \pi, \pi, 3\pi/2)$.

It follows that for all cases in Table 1 we have $n_+ \geq 1$. Therefore, all equilibria are unstable, and asymptotic stability occurs only for the total synchrony subspace in the sense of Lyapunov as given in the previous subsection.

5.4.3 A homogeneous network \tilde{G}_6 with two types of couplings

The aim of this example is to illustrate that there are stable equilibria from a ‘modification’ of G_6 . We consider a network system with six cells and coupling defined from the graph \tilde{G}_6 given in Fig. 12. The symmetry group of this graph is

$$\text{Aut}(\tilde{G}_6) = \mathbb{Z}_2^1 \times \mathbb{Z}_2^2 \times \mathbb{Z}_3,$$

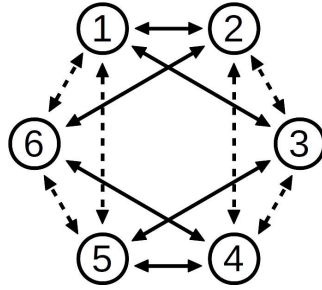
where $\mathbb{Z}_2^1 = \langle (15)(24) \rangle$ and $\mathbb{Z}_2^2 = \langle (12)(36)(45) \rangle$, which are not conjugate, and $\mathbb{Z}_3 = \langle (156)(234) \rangle$.

We choose the coupling functions $\phi(\theta) = \sin \theta$, which is represented by the continuous arrow type in Fig. 12, and $\psi(\theta) = \theta$, represented by the dashed arrow type, so the network system is

$$\begin{aligned} \dot{x}_1 &= \sin(x_2 - x_1) + \sin(x_3 - x_1) + x_5 + x_6 - 2x_1 \\ \dot{x}_2 &= \sin(x_1 - x_2) + \sin(x_6 - x_2) + x_3 + x_4 - 2x_2 \\ \dot{x}_3 &= \sin(x_1 - x_3) + \sin(x_5 - x_3) + x_2 + x_4 - 2x_3 \\ \dot{x}_4 &= \sin(x_5 - x_4) + \sin(x_6 - x_4) + x_2 + x_3 - 2x_4 \\ \dot{x}_5 &= \sin(x_3 - x_5) + \sin(x_4 - x_5) + x_1 + x_6 - 2x_5 \\ \dot{x}_6 &= \sin(x_2 - x_6) + \sin(x_4 - x_6) + x_1 + x_5 - 2x_6 \end{aligned}$$

By direct investigation from the output of our code (Remark 3.2), there are no exotic synchrony patterns in this network graph.

The analysis follows analogously as in the previous subsection, so we shall just present a summary with the results. The diagram in (5.19) is the lattice of non-trivial synchrony subspace up to conjugacy.

Figure 12 – A homogeneous \tilde{G}_6

$$\begin{array}{ccc}
 \text{Fix}\langle(156)(234)\rangle & \longrightarrow & \text{Fix}\langle(15)(24)\rangle \\
 & \searrow & \\
 \text{Fix}\langle(12)(36)(45), (15)(24)\rangle & \longrightarrow & \text{Fix}\langle(12)(36)(45)\rangle \\
 & \searrow & \\
 & & \text{Fix}\langle(14)(25)(36)\rangle
 \end{array} \tag{5.19}$$

For $\Sigma = \langle(15)(24)\rangle$, we search for critical points of the form $(0, a, b, a, 0, c)$, for $a, b, c, \in \mathbb{R}$:

$$\begin{aligned}
 \sin(-a) + \sin(c - a) + (b - a) &= 0 \\
 2(a - b) + 2\sin(-b) &= 0 \\
 -2c + \sin(a - c) &= 0,
 \end{aligned}$$

which imply that

$$\sin b + b = a = c + \arcsin c,$$

Since $t \mapsto \sin(t) + t$ is injective, then $c = \sin b$. Together with the first equality, this gives $\sin a = -2\sin b$, and so $\sin(b + \sin b) + 2\sin b = 0$. Hence, $b = k\pi, k \in \mathbb{Z}$, and also $a = b$. Therefore, the critical points are

$$(0, k\pi, k\pi, k\pi, 0, 0), \quad k \in \mathbb{Z}.$$

For $\Sigma = \langle(14)(25)(36)\rangle$, we search for critical points of the form $(0, a, b, 0, a, b)$, $a, b \in \mathbb{R}$:

$$\begin{aligned}
 \sin a + \sin b + a + b &= 0 \\
 \sin(b - a) + \sin(-a) - 2b + a &= 0,
 \end{aligned}$$

which imply that $\sin a + a = \sin(-b) - b$, and then $a = -b$. Together with the second equality, this gives $\sin(2a) + 2a = \sin(-a) - a$, and then $a = b = 0$. This gives the total synchrony, which has already been considered.

For $\Sigma = \langle(12)(36)(45)\rangle$, we search for critical points of the form $(a, a, 0, b, b, 0)$, $a, b \in \mathbb{R}$:

$$\begin{aligned}
 b &= 2a + \sin a \\
 a &= 2b + \sin b,
 \end{aligned}$$

which also imply $a = b = 0$. It follows from the computation of n_+ and n_- by Theorem 5.1 that $(0, k\pi, k\pi, k\pi, 0, 0)$ is a one parameter family of stable equilibria for k even and unstable if k is odd.

#	Critical point representative	$c(G_+)$	$c(G_-)$	$c(G)$	$n_+(L)$
1	-	-	-	-	-
2	$(0, 0, \pi, 0, 0, 0)$	2	2	1	$1 \leq n_+ \leq 4$
3	$(0, 0, \alpha, \pi, \pi, -\alpha)$ $(0, 0, \alpha, \pi, \pi, \alpha + \pi)$ $\alpha \neq 0, \pi, \pm \frac{\pi}{2}$	2	1	1	$1 \leq n_+ \leq 5$
3	$(0, 0, \pm \frac{\pi}{2}, \pi, \pi, \mp \frac{\pi}{2})$ $(0, 0, \pm \frac{\pi}{2}, \pi, \pi, \pm \frac{\pi}{2} + \pi)$	4	4	3	$1 \leq n_+ \leq 2$
4	$(0, \pi, \alpha, 0, \pi, -\alpha)$ $(0, \pi, \alpha, 0, \pi, \alpha + \pi)$ $\alpha \neq 0, \pi, \pm \frac{\pi}{2}$	2	1	1	$1 \leq n_+ \leq 5$
4	$(0, \pi, \pm \frac{\pi}{2}, 0, \pi, \mp \frac{\pi}{2})$ $(0, \pi, \pm \frac{\pi}{2}, 0, \pi, \pm \frac{\pi}{2} + \pi)$	6	3	3	$3 \leq n_+ \leq 3$
4	$(0, \pi, \pi, 0, \pi, 0)$	2	2	1	$1 \leq n_+ \leq 4$
5	$(0, \pi, 0, 0, \pi, 0)$	3	1	1	$2 \leq n_+ \leq 5$
6	$(0, 0, 0, \pi, \pi, \pi)$	2	1	1	$1 \leq n_+ \leq 5$
7	$(0, 0, 0, \pi, \pi, 0)$	2	1	1	$1 \leq n_+ \leq 5$
8	$(0, \frac{4\pi}{3}, \frac{2\pi}{3}, 0, \frac{4\pi}{3}, \frac{2\pi}{3})$	6	1	1	$5 \leq n_+ \leq 5$

Table 3 – The first column indicate the synchrony patterns extracted from Table 1; the corresponding class of critical points is given in the second column by a representative up to the symmetries of $Aut(G_6)$; the last column gives the number n_+ of positive eigenvalues of the Jacobian at the corresponding critical point; the remaining three columns are the data used to apply Theorem 5.1.

FUTURE RESEARCH

- One possible next step of this research is to try to obtain similar results of ([JADBABAIE; MOTEE; BARAHONA, 2004](#); [BRONSKI; CARTY; DEVILLE, 2021](#)) for Laplacian maps plus a vector of non-identical natural frequencies. The idea is look for conditions on the natural frequencies for the existence of critical points and then study their stabilities.
- In [Theorem 3.3](#) we give sufficient condition for a polydiagonal invariant subspace to be a synchrony subspace of an admissible graph. We guess that it is possible to find necessary conditions for this.
- We also want to find an example of a Laplacian mapping that displays analytically a stable chimera state. It was done numerically for Kuramoto model in ([KOTWAL; JIANG; ABRAMS, 2017](#)).
- As [Corollary 5.11](#) shows, a Laplacian mapping is gradient. We intend to study Hamiltonian systems $\dot{x} = J\nabla g$, where J is the standard anti-symmetric orthogonal matrix and g is as in [Corollary 5.11](#). We believe that there may be a closer relation between admissible graphs in the two context possibly given by the role of matrix J connection to two algebraic form of vector field.

BIBLIOGRAPHY

ABRAMS, D. M.; STROGATZ, S. H. Chimera states in a ring of nonlocally coupled oscillators. **International Journal of Bifurcation and Chaos**, World Scientific, v. 16, n. 01, p. 21–37, 2006. Citations on pages [22](#) and [50](#).

ACEBRÓN, J. A.; BONILLA, L. L.; VICENTE, C. J. P.; RITORT, F.; SPIGLER, R. The kuramoto model: A simple paradigm for synchronization phenomena. **Reviews of modern physics**, APS, v. 77, n. 1, p. 137, 2005. Citation on page [22](#).

AGUIAR, M. A.; DIAS, A. P. S. The lattice of synchrony subspaces of a coupled cell network: Characterization and computation algorithm. **Journal of Nonlinear Science**, Springer, v. 24, p. 949–996, 2014. Citations on pages [20](#), [25](#), [32](#), [75](#), and [76](#).

AMORIM, T.; MANOEL, M. The realization of admissible graphs for coupled vector fields. **arXiv preprint arXiv:2212.07537**, 2022, accepted in 14 November 2023 by Nonlinearity, IOP Publishing. Citations on pages [25](#) and [37](#).

_____. Synchrony patterns in laplacian networks. **arXiv preprint arXiv:2308.09097**, 2023. Citations on pages [25](#), [31](#), and [55](#).

ANTONELLI, F.; STEWART, I. Symmetry and synchrony in coupled cell networks 1: Fixed-point spaces. **International Journal of Bifurcation and Chaos**, World Scientific, v. 16, n. 03, p. 559–577, 2006. Citations on pages [20](#), [24](#), [33](#), [35](#), and [63](#).

BRACIKOWSKI, C.; ROY, R. Chaos in a multimode solid-state laser system. **Chaos: An Interdisciplinary Journal of Nonlinear Science**, American Institute of Physics, v. 1, n. 1, p. 49–64, 1991. Citation on page [19](#).

BRONSKI, J. C.; CARTY, T. E.; DEVILLE, L. Synchronisation conditions in the kuramoto model and their relationship to seminorms. **Nonlinearity**, IOP Publishing, v. 34, n. 8, p. 5399, 2021. Citations on pages [23](#) and [69](#).

BRONSKI, J. C.; DEVILLE, L. Spectral theory for dynamics on graphs containing attractive and repulsive interactions. **SIAM Journal on Applied Mathematics**, SIAM, v. 74, n. 1, p. 83–105, 2014. Citations on pages [23](#), [55](#), and [56](#).

CHANDRASEKAR, V.; GOPAL, R.; VENKATESAN, A.; LAKSHMANAN, M. Mechanism for intensity-induced chimera states in globally coupled oscillators. **Physical Review E**, APS, v. 90, n. 6, p. 062913, 2014. Citation on page [50](#).

CZAJKOWSKI, B. M.; BATISTA, C. A.; VIANA, R. L. Synchronization of phase oscillators with chemical coupling: Removal of oscillators and external feedback control. **Physica A: Statistical Mechanics and its Applications**, Elsevier, v. 610, p. 128418, 2023. Citation on page [23](#).

DIAS, A. P. S.; STEWART, I. Linear equivalence and ode-equivalence for coupled cell networks. **Nonlinearity**, IOP Publishing, v. 18, n. 3, p. 1003, 2005. Citations on pages [20](#) and [30](#).

FOWLES, G. R.; CASSIDAY, G. L. *et al.* **Analytical mechanics**. [S.l.: s.n.], 1986. Citation on page 19.

GOLUBITSKY, M.; NICOL, M.; STEWART, I. Some curious phenomena in coupled cell networks. **Journal of Nonlinear Science**, Springer, v. 14, p. 207–236, 2004. Citations on pages 19, 33, and 51.

GOLUBITSKY, M.; STEWART, I. **The symmetry perspective: from equilibrium to chaos in phase space and physical space**. [S.l.]: Springer Science & Business Media, 2003. Citation on page 19.

GOLUBITSKY, M.; STEWART, I.; TÖRÖK, A. Patterns of synchrony in coupled cell networks with multiple arrows. **SIAM Journal on Applied Dynamical Systems**, SIAM, v. 4, n. 1, p. 78–100, 2005. Citations on pages 19, 20, 27, 31, 32, and 37.

HADLEY, P.; BEASLEY, M.; WIESENFELD, K. Phase locking of josephson-junction series arrays. **Physical Review B**, APS, v. 38, n. 13, p. 8712, 1988. Citation on page 19.

JADBABAIE, A.; MOTEE, N.; BARAHONA, M. On the stability of the kuramoto model of coupled nonlinear oscillators. In: IEEE. **Proceedings of the 2004 American Control Conference**. [S.l.], 2004. v. 5, p. 4296–4301. Citations on pages 24 and 69.

KOPELL, N.; ERMENTROUT, G. Phase transitions and other phenomena in chains of coupled oscillators. **SIAM Journal on Applied Mathematics**, SIAM, v. 50, n. 4, p. 1014–1052, 1990. Citation on page 19.

KOPELL, N.; ERMENTROUT, G. B. Symmetry and phaselocking in chains of weakly coupled oscillators. **Communications on Pure and Applied Mathematics**, Wiley Online Library, v. 39, n. 5, p. 623–660, 1986. Citation on page 19.

_____. Coupled oscillators and the design of central pattern generators. **Mathematical biosciences**, Elsevier, v. 90, n. 1-2, p. 87–109, 1988. Citation on page 19.

KOTWAL, T.; JIANG, X.; ABRAMS, D. M. Connecting the kuramoto model and the chimera state. **Physical review letters**, APS, v. 119, n. 26, p. 264101, 2017. Citations on pages 23 and 69.

KURAMOTO, Y. Self-entrainment of a population of coupled non-linear oscillators. In: SPRINGER. **International Symposium on Mathematical Problems in Theoretical Physics: January 23–29, 1975, Kyoto University, Kyoto/Japan**. [S.l.], 1975. p. 420–422. Citation on page 22.

KURAMOTO, Y.; BATTOGTOKH, D. Coexistence of coherence and incoherence in nonlocally coupled phase oscillators. **arXiv preprint cond-mat/0210694**, 2002. Citations on pages 22 and 50.

MANOEL, M.; ROBERTS, M. Gradient systems on coupled cell networks. **Nonlinearity**, IOP Publishing, v. 28, n. 10, p. 3487, 2015. Citations on pages 23, 24, and 34.

MARTENS, E. A.; THUTUPALLI, S.; FOURRIERE, A.; HALLATSCHEK, O. Chimera states in mechanical oscillator networks. **Proceedings of the National Academy of Sciences**, National Acad Sciences, v. 110, n. 26, p. 10563–10567, 2013. Citation on page 22.

NOVIKOV, A.; BENDERSKAYA, E. Oscillatory neural networks based on the kuramoto model for cluster analysis. **Pattern recognition and image analysis**, Springer, v. 24, p. 365–371, 2014. Citation on page [23](#).

PANAGGIO, M. J.; ABRAMS, D. M. Chimera states: coexistence of coherence and incoherence in networks of coupled oscillators. **Nonlinearity**, IOP Publishing, v. 28, n. 3, p. R67, 2015. Citation on page [22](#).

SIMO, G. R.; NJOUGOUO, T.; ARISTIDES, R.; LOUODOP, P.; TCHITNGA, R.; CERDEIRA, H. A. Chimera states in a neuronal network under the action of an electric field. **Physical Review E**, APS, v. 103, n. 6, p. 062304, 2021. Citation on page [22](#).

STEPHAN, W. Griffiths, J.B., the theory of classical dynamics. Cambridge etc., Cambridge University Press 1985. xiv, 315 s., £ 20, 00, 39.50. *isbn0 – 521 – 23760 – 2. Zeitschrift Angewandte Mathematik und Mechanik*, v. 67, n. 1, p. 36 – 36, 1987. Citation on page [19](#).

STEWART, I.; ELMHIRST, T.; COHEN, J. Symmetry-breaking as an origin of species. In: **Bifurcation, symmetry and patterns**. [S.l.]: Springer, 2003. p. 3–54. Citation on page [19](#).

STEWART, I.; GOLUBITSKY, M.; PIVATO, M. Symmetry groupoids and patterns of synchrony in coupled cell networks. **SIAM Journal on Applied Dynamical Systems**, SIAM, v. 2, n. 4, p. 609–646, 2003. Citations on pages [19](#), [20](#), [27](#), [28](#), [31](#), and [37](#).

VANDERMEER, J.; HAJIAN-FOROOSHANI, Z.; MEDINA, N.; PERFECTO, I. New forms of structure in ecosystems revealed with the kuramoto model. **Royal Society open science**, The Royal Society, v. 8, n. 3, p. 210122, 2021. Citation on page [23](#).

WANG, S.; WINFUL, H. G. Dynamics of phase-locked semiconductor laser arrays. **Applied physics letters**, American Institute of Physics, v. 52, n. 21, p. 1774–1776, 1988. Citation on page [19](#).

WIGGINS, S. Introduction to applied nonlinear dynamical systems and chaos, 2003 (texts in applied mathematics). 2003. Citation on page [61](#).

ZAKHAROVA, A. Chimera patterns in networks. **Springer**, Springer, 2020. Citation on page [22](#).

ALGORITHM TO LIST SYNCHRONY SUBSPACES FOR BIDIRECTED REGULAR NETWORKS

Here we explain our implementation of algorithm presented in (AGUIAR; DIAS, 2014), but first we present briefly the theoretical basis for this algorithm.

Given a network graph \mathcal{G} with n cell, by (3.2) a synchrony subspace is a subspace of \mathbb{R}^n invariant under all adjacency matrix. So the idea is search for polydiagonal subspaces that is invariant under each one of adjacency matrices, and then select these ones is common for all matrices. See (AGUIAR; DIAS, 2014, Theorem 4.2).

Now suppose that \mathcal{G} is regular with only one matrix A . Our work is list all invariant subspaces that satisfy equalities of the type $x_i = x_j$, so we have to look at sets of eigenvectors and take note of equalities that they satisfy. By (AGUIAR; DIAS, 2014, Theorem 5.13) a polydiagonal subspace is a synchrony subspace if admit a base of eigenvectors. Then we get together the eigenvectors that satisfy the same set of equalities and if these vectors form a base of subspace defined by this set of equalities, then we have a synchrony subspace.

If A is not symmetric, that is, \mathcal{G} is not bidirected, perhaps we need to consider generalized eigenvector and treat them apart getting more complexity to steps of algorithm. Few of our examples needed this part, in these cases we did it manually. So we have implemented the algorithm just to regular bidirected connected network graph and the unique initial data is the symmetric adjacency matrix.

Throughout the process the code produce a list of elements having five entries: The first one is a set of equalities of form $x_i = x_j$, the second one is the dimension of subspace defined by these equations, the third one is the number of equations, the fourth one is a set of eigenvectors that satisfy this equations and the last one is the dimension of subspace generated by these

vectors. As the vector $(1, 1, \dots, 1)$ is even a eigenvector of A , once all rows of A has the same sum, and it satisfies any set of equalities we omit this data in the code. Then if a element of this list has the fifth entry equal to do second entry minus 1, this element indicate a synchrony subspace.

Our code is divided into four parts:

Part 1: Computes the eigenvalues and for each them gives a set of linearly independent eigenvector and take note the equalities satisfied by that.

Part 2: The rows of matrix $MBar$ is the difference between rows of matrix of eigenvectors. By (AGUIAR; DIAS, 2014, Lemma 6.1) if we want eigenvector that satisfy, for example, $x_1 = x_3 = x_7$, we need do compute the kernel of submatrix of $MBar$ formed by difference of rows 1, 3 and 7 of matrix of eigenvectors computed in the part 1. So for each eigenvalue, this part computes the kernel of all submatrices of $MBar$ and create elements with five entries as mentioned above.

Part 3: Gets together the eigenvectors that satisfy the same set of equalities and then select the synchrony subspaces.

Part 4: Turns the final list into a better layout.

The part 1 of code:

```
AdjMatrix = (* PUT HERE THE THE ADJACENCY MATRIX*);
n = Length[AdjMatrix];
valencia = Sum[AdjMatrix[[1, j]], {j, 1, n}];
eigenvalues = Complement[Union[Eigenvalues[AdjMatrix]], {valencia}]
lengtheigenvalues = Length[eigenvalues];
eigenvectors =
  Table[Transpose[
    NullSpace[AdjMatrix - eigenvalues[[ev]]*IdentityMatrix[n]], {ev,
      1, lengtheigenvalues}];
listaux1a = Subsets[Range[n], {2}];
sizelistaux1a = Length[listaux1a];
g1 = If[eigenvectors[[ev, #1]] == eigenvectors[[ev, #2]] ,
  Subscript[x, #1] == Subscript[x, #2], Null] &;
gg1 = Apply[g1, {listaux1a[[#, 1]], listaux1a[[#, 2]]}] &;
g2 = If[eigenvectors[[ev, #1]] == eigenvectors[[ev, #2]], {#1, #2},
  Null] &;
gg2 = Apply[g2, {listaux1a[[#, 1]], listaux1a[[#, 2]]}] &;
listcondition =
```

```

Table[Complement[Array[gg2, sizelistaux1a], {Null}], {ev, 1,
  lengtheigenvalues}];
Conditioninicial =
Table[Complement[Array[gg1, sizelistaux1a], {Null}], {ev, 1,
  lengtheigenvalues}];
sizelistcondition =
Table[Length[listcondition[[ev]]], {ev, 1, lengtheigenvalues}];
g3 = listcondition[[ev, #, 1]] &;
g4 = listcondition[[ev, #, 2]] &;
list1 = Table[
  Union[Complement[Array[g3, sizelistcondition[[ev]]],
    Array[g4, sizelistcondition[[ev]]]],
  Complement[Range[n],
    Union[Array[g3, sizelistcondition[[ev]]],
    Array[g4, sizelistcondition[[ev]]]]], {ev, 1,
  lengtheigenvalues}];

```

The part 2 of code:

```

M1 = Table[
  eigenvectors[[ev, list1[[ev]]]], {ev, 1, lengtheigenvalues}];
sizelist1 = Table[Length[list1[[ev]]], {ev, 1, lengtheigenvalues}];
list2 = Table[
  Subsets[Range[sizelist1[[ev]]], {2}], {ev, 1,
  lengtheigenvalues}];
sizelist2 = Table[Length[list2[[ev]]], {ev, 1, lengtheigenvalues}];
f12 = M1[[ev, #1]] - M1[[ev, #2]] &;
f13 = Apply[f12, {list2[[ev, #1, 1]
], list2[[ev, #1, 2]]}] &;
Mbar = Table[
  Simplify[Array[f13, {sizelist2[[ev]]}], {ev, 1,
  lengtheigenvalues}];
Table[MatrixForm[Mbar[[ev]]], {ev, 1, lengtheigenvalues}];
nullspacef0 = NullSpace[{Mbar[[ev, #]]}] &;
nullspacelist0 =
Table[Array>nullspacef0, sizelist2[[ev]]], {ev, 1,
  lengtheigenvalues}];
listfinalf0 =
If[sizelist2[[ev]] ==
  1, {}, {Union[

```

```

Conditioninicial[[
  ev]], {Subscript[x, list1[[ev, list2[[ev, #, 1]]]]] ==
  Subscript[x, list1[[ev, list2[[ev, #, 2]]]]]}},
n - If[Length[Conditioninicial[[ev]]] == 0, 1,
  Length[Reduce[
    Union[Conditioninicial[[
      ev]], {Subscript[x, list1[[ev, list2[[ev, #, 1]]]]] ==
      Subscript[x, list1[[ev, list2[[ev, #, 2]]]]]}]]],
Length[Union[
  Conditioninicial[[
    ev]], {Subscript[x, list1[[ev, list2[[ev, #, 1]]]]] ==
    Subscript[x, list1[[ev, list2[[ev, #, 2]]]]]}]]],
Table[Simplify[
  Sum[nullspacelist0[[ev, #, j, k]]*
    eigenvectors[[ev, All, k]], {k, 1,
    Length[eigenvectors[[ev, 1]]]}], {j, 1,
    Length[nullspacelist0[[ev, #]]]}],
  Length[eigenvectors[[ev, 1]] - 1] &;
listfinal0 =
Table[Array[listfinalf0, sizelist2[[ev]]], {ev, 1,
  lengtheigenvalues}] ;
listfinal00 =
Table[{{Conditioninicial[[ev]], sizelist1[[ev]],
  sizelistcondition[[ev]],
  Table[eigenvectors[[ev, All, i]], {i, 1,
    Length[eigenvectors[[ev, 1]]]}],
  Length[eigenvectors[[ev, 1]]]}}, {ev, 1, lengtheigenvalues}];
Subscript[listaux, 1] =
Table[Subsets[Range[sizelist2[[ev]]], {2}], {ev, 1,
  lengtheigenvalues}];
Subscript[sizelistaux, 1] =
Table[Length[Subscript[listaux, 1][[ev]]], {ev, 1,
  lengtheigenvalues}];
Subscript[testRankf, 1] =
MatrixRank[Mbar[[ev, Subscript[listaux, 1][[ev, #]]]]] & ;
Subscript[testRanklist, 1] =
Table[Array[Subscript[testRankf, 1],
  Subscript[sizelistaux, 1][[ev]]], {ev, 1, lengtheigenvalues}];
Subscript[testRanklista, 1] =

```

```

Table[Union[
  Flatten[Table[
    Flatten[Position[Subscript[testRanklist, 1][[ev]], j], 1], {j,
      1, Length[eigenvalues[[ev, 1]] - 1] 1}], {ev, 1,
    lengtheigenvalues}];
Subscript[sizetestRanklista, 1] =
  Table[Length[Subscript[testRanklista, 1][[ev]]], {ev, 1,
    lengtheigenvalues}];
Subscript[nullspacef, 1] =
  NullSpace[
    Mbar[[ev,
      Subscript[listaux, 1][[ev,
        Subscript[testRanklista, 1][[ev, #]]]]]] &;
Subscript[nullspacelist, 1] =
  Table[If[Subscript[testRanklista, 1][[ev]] == {}, {},
    Array[Subscript[nullspacef, 1],
      Subscript[sizetestRanklista, 1][[ev]]], {ev, 1,
    lengtheigenvalues}];
Subscript[newlistcondition, 1] =
  Table[If[Subscript[testRanklista, 1][[ev]] == {}, {},
    Table[Union[
      Conditioninicial[[
        ev]], {Subscript[x,
        list1[[ev,
        list2[[ev,
        Subscript[listaux, 1][[ev,
        Subscript[testRanklista, 1][[ev, j]], 1]], 1]]]] ==
      Subscript[x,
        list1[[ev,
        list2[[ev,
        Subscript[listaux, 1][[ev,
        Subscript[testRanklista, 1][[ev, j]], 1]], 2]]]],
      Subscript[x,
        list1[[ev,
        list2[[ev,
        Subscript[listaux, 1][[ev,
        Subscript[testRanklista, 1][[ev, j]], 2]], 1]]]] ==
      Subscript[x,
        list1[[ev,

```

```

list2[[ev,
Subscript[listaux, 1][[ev,
Subscript[testRanklista, 1][[ev, j]], 2]], 2]]], {j, 1,
Subscript[sizetestRanklista, 1][[ev]]}], {ev, 1,
lengtheigenvalues}];
Subscript[listfinalf,
1] = {Subscript[newlistcondition, 1][[ev, #]],
n - Length[Reduce[Subscript[newlistcondition, 1][[ev, #]]],
Length[Subscript[newlistcondition, 1][[ev, #]]],
Table[Simplify[
Sum[Subscript[nullspacelist, 1][[ev, #, j, k]]*
eigenvectors[[ev, All, k]], {k, 1,
Length[eigenvectors[[ev, 1]]}], {j, 1,
Length[Subscript[nullspacelist, 1][[ev, #]]}],
Length[Subscript[nullspacelist, 1][[ev, #]]} &];
Subscript[listfinal, 1] =
Table[If[Subscript[testRanklista, 1][[ev]] == {}, {},
Array[Subscript[listfinalf, 1],
Subscript[sizetestRanklista, 1][[ev]]], {ev, 1,
lengtheigenvalues}];
j = 2; While[
Union[Subscript[testRanklistaa, j]] != {} \[Or] j <= Max[sizelist2],
{Subscript[listauxha, j] =
If[j == 2,
Table[If[Subscript[testRanklista, 1][[ev]] == {}, {},
Table[Subscript[listaux, 1][[ev,
Subscript[testRanklista, 1][[ev, 1]]]], {1, 1,
Length[Subscript[testRanklista, 1][[ev]]}], {ev, 1,
lengtheigenvalues}],
Table[If[Subscript[testRanklistaa, j - 1][[ev]] == {}, {},
Table[Subscript[listauxa, j - 1][[ev,
Subscript[testRanklistaa, j - 1][[ev, 1]]]], {1, 1,
Length[Subscript[testRanklistaa, j - 1][[ev]]}], {ev, 1,
lengtheigenvalues}]]],
Subscript[hfa, j][1_] =
Union[Subscript[listauxha, j][[ev, 1]], {#}] &,
Subscript[listauxa, j] =
Table[Union[
Cases[Flatten[

```

```

Table[Array[Subscript[hfa, j][1], sizelist2[[ev]]], {1, 1,
  Length[Subscript[listauxha, j][[ev]]]}, 1],
Table[_, j + 1]], {ev, 1, lengtheigenvalues}},
Subscript[sizelistauxa, j] =
Table[Length[Subscript[listauxa, j][[ev]]], {ev, 1,
  lengtheigenvalues}},
Subscript[testRankfa, j] =
MatrixRank[Mbar[[ev, Subscript[listauxa, j][[ev, #]]]]] &,
Subscript[testRanklista, j] =
Table[Array[Subscript[testRankfa, j],
  Subscript[sizelistauxa, j][[ev]]], {ev, 1, lengtheigenvalues}},
Subscript[testRanklistaa, j] =
Table[Union[
  Flatten[Table[
    Flatten[Position[Subscript[testRanklista, j][[ev]], 1],
    1], {1, 1, Length[eigenvectors[[ev, 1]]] - 1} 1]], {ev, 1,
  lengtheigenvalues}] ,
Subscript[sizetestRanklista, j] =
Table[Length[Subscript[testRanklistaa, j][[ev]]], {ev, 1,
  lengtheigenvalues}] ,
Subscript[nullspacefa, j] =
NullSpace[
  Mbar[[ev,
    Subscript[listauxa, j][[ev,
    Subscript[testRanklistaa, j][[ev, #]]]]]]] &,
Subscript[nullspacefa, j] =
Table[If[Subscript[sizetestRanklista, j][[ev]] == 0, {},
  Array[Subscript[nullspacefa, j],
    Subscript[sizetestRanklista, j][[ev]]], {ev, 1,
  lengtheigenvalues}] ,
Subscript[newlistconditiona, j] =
Table[If[Subscript[sizetestRanklista, j][[ev]] == 0, {},
  Table[Flatten[{Union[
    Conditioninicial[[
      ev]], {Table[
        Subscript[x,
          list1[[ev,
            list2[[ev,

```

```

Subscript[listauxa, j][[ev,
  Subscript[testRanklistaa, j][[ev, 1]], k]], 1]]] ==
Subscript[x,
list1[[ev,
list2[[ev,
  Subscript[listauxa, j][[ev,
    Subscript[testRanklistaa, j][[ev, 1]], k]], 2]]]], {k,
  1, j + 1}}]], {1, 1,
  Subscript[sizetestRanklista, j][[ev]]}], {ev, 1,
  lengtheigenvalues}],
Subscript[listfinalfa,
j] = {Subscript[newlistconditiona, j][[ev, #]],
  n - Length[Reduce[Subscript[newlistconditiona, j][[ev, #]]],
Length[Subscript[newlistconditiona, j][[ev, #]]],
  Table[Simplify[
    Sum[Subscript[nullspacelista, j][[ev, #, 1, k]]*
    eigenvectors[[ev, All, k]], {k, 1,
    Length[eigenvectors[[ev, 1]]}], {1, 1,
    Length[Subscript[nullspacelista, j][[ev, #]]}],
Length[Subscript[nullspacelista, j][[ev, #]]] &,
  Subscript[listfinala, j] =
Table[If[Subscript[sizetestRanklista, j][[ev]] == 0, {},
  Array[Subscript[listfinalfa, j],
    Subscript[sizetestRanklista, j][[ev]]], {ev, 1,
  lengtheigenvalues}]]; j++];
AAA = Union[
Flatten[Table[Flatten[Subscript[listfinala, 1], 1], {1, 2, j - 1}],
  1]];
listFinal1 =
Complement[
  Union[Flatten[Subscript[listfinal, 1], 1], AAA,
  Flatten[listfinal0, 1], Flatten[listfinal00, 1]], {{}}]
listvariables = Table[Subscript[x, 1], {1, 1, n}];
listallequalities =
  Flatten[Table[
    Subscript[x, 1] == Subscript[x, k], {1, 1, n - 1}, {k, 1 + 1, n}],
  1];
sizelistallequalities = Length[listallequalities];
funccompletingequations[l_] =

```

```

If[Reduce[listFinal1[[1, 1]], listvariables] ==
  Reduce[Union[listFinal1[[1, 1]], {listallequalities[[#]]}],
  listvariables], listallequalities[[#]], Null, Null] &;
completingequations =
Table[Complement[
  Array[funccompletingequations[1],
    sizelistallequalities], {Null}], {1, 1, Length[listFinal1]};
list2f = {completingequations[[#]], listFinal1[[#, 2]],
Length[completingequations[[#]]], listFinal1[[#, 4]],
  listFinal1[[#, 5]]} &;
listFinal2 = SortBy[Union[Array[list2f, Length[listFinal1]]], First];
sizelistFinal1 = Length[listFinal1]
sizelistFinal2 = Length[listFinal2]
balancedrelationinicial =
  Union[Flatten[
    Table[Cases[listFinal2, {_, 1, _, _, 1 - 1}], {1, 2, n}], 1]] ;
AAAA = Complement[listFinal2, balancedrelationinicial];
M = Max[Table[AAAA[[1, 3]], {1, 1, Length[AAAA]}]];

```

The part 3 of code:

```

jj = -1; While[
jj < M - 1, {Subscript[l1, jj] =
  If[jj == -1, {}, Subscript[newlist, jj - 1]],
Subscript[sizell, jj] = Length[Subscript[l1, jj]],
Subscript[complement, jj][
  l_] = {Complement[
  Subscript[l1, jj][[1, 1]], {Subscript[l1, jj][[1, 1, #]]}},
  n - Length[
  Reduce[Complement[
    Subscript[l1, jj][[1, 1]], {Subscript[l1, jj][[1, 1, #]]}],
  Subscript[l1, jj][[1, 3]] - 1, Subscript[l1, jj][[1, 4]],
  Subscript[l1, jj][[1, 5]]} &,
Subscript[l11, jj] =
  Union[Flatten[
Table[Array[Subscript[complement, jj][i], M - jj], {i, 1,
  Subscript[sizell, jj]}], 1],
  Cases[listFinal2, {_, _, M - jj - 1, _, _}],
Subscript[l12, jj] =
  Union[Flatten[

```

```

Union[Table[
  Cases[listFinal2, {_, _, 1, _, _}], {1,
    Range[M - jj - 1, sizelistallequalities]]], 1]],
Subscript[sizell1, jj] = Length[Subscript[l11, jj]],
Subscript[sizell2, jj] = Length[Subscript[l12, jj]],
Subscript[ffg, jj][1_] =
If[Reduce[Subscript[l12, jj][[#, 1]], listvariables] ==
  Reduce[Union[Subscript[l12, jj][[#, 1]],
    Subscript[l11, jj][[1, 1]]], listvariables], #, Null,
Null] &,
Subscript[g2a, jj] =
Table[Complement[
  Array[Subscript[ffg, jj][1], Subscript[sizell2,
    jj]], {Null}], {1, 1, Subscript[sizell1, jj]}],
Subscript[aaf, jj] =
Union[Flatten[
  Table[Subscript[l12, jj][[Subscript[g2a, jj][[#, i]], 4]], {i,
    1, Length[Subscript[g2a, jj][[#]]}], 1]] &,
Subscript[aa, jj] =
Array[Subscript[aaf, jj], Subscript[sizell1, jj]],
Subscript[newlistf,
jj] = {Subscript[l11, jj][[#, 1]],
  n - If[jj == M - 2, 1,
    Length[Reduce[Subscript[l11, jj][[#, 1]]]], M - jj - 1,
  Subscript[aa, jj][[#]], MatrixRank[Subscript[aa, jj][[#]]]} &,
Subscript[newlist, jj] =
Union[Array[Subscript[newlistf, jj], Subscript[sizell1, jj]],
Print[Length[Subscript[newlist, jj]]]; jj++];
newlistT =
Union[Flatten[Table[Subscript[newlist, 1], {1, -1, M - 2}], 1]];
balancedrelationfinal =
Union[Flatten[
  Table[Cases[newlistT, {_, 1, _, _, 1 - 1}], {1, 2, n}], 1]] ;
balancedrelationA =
Union[balancedrelationinicial, balancedrelationfinal];
sizebalancedrelationA = Length[balancedrelationA];

```

The part 4 of code:

```

funccompletingequations2[l_] =

```

```

If[Reduce[balancedrelationA[[1, 1]], listvariables] ==
  Reduce[Union[
    balancedrelationA[[1, 1]], {listallequalities[[#]]}],
  listvariables], listallequalities[[#]], Null, Null] &;
completingequations2 =
  Table[Complement[
Array[funccompletingequations2[1],
  sizelistallequalities], {Null}], {1, 1,
  Length[balancedrelationA]}];
list2f2 = {completingequations2[[#]], balancedrelationA[[#, 2]],
Length[completingequations2[[#]]], balancedrelationA[[#, 4]],
  balancedrelationA[[#, 5]]} &;
list22 = SortBy[Array[list2f2, Length[balancedrelationA]], First];
BB = Union[
  Flatten[Table[Cases[list22, {_, i, _, _, _}], {i, 2, n - 2}], 1]];
BB1 = Table[BB[[i, 1]], {i, 1, Length[BB]}];
BB2 = Table[
  Table[{BB1[[k, i, 1]], BB1[[k, i, 2]]}, {i, 1,
    Length[BB1[[k]]}], {k, 1, Length[BB1]}];
rBB1 = Table[Reduce[BB1[[k]], listvariables], {k, 1, Length[BB1]}];
f2[k_] = rBB1[[k, #, 2]] &;
h2 = Table[
  Union[Array[f2[k], Length[rBB1[[k]]]], {k, 1, Length[BB1]}];
V = Cases[finallistbalanced, {_, n - 1, _, _, _}];
newBB2 =
  Union[Table[{{V[[k, 1]][[1]][[1]], V[[k, 1]][[1]][[2]]}}, {k, 1,
    Length[V]}],
  Table[Table[
    Union[Flatten[Cases[BB2[[k]], {h2[[k, i]], _}], 1]], {i, 1,
      Length[h2[[k]]}], {k, 1, Length[BB1]}];
S[k_, l_] = newBB2[[k, l, #]] &;
newBB3 =
  Table[ Table[
    Array[S[k, l], {Length[newBB2[[k, l]]}], 1, Equal], {1, 1,
      Length[newBB2[[k]]}], {k, 1, Length[newBB2]}];
MatrixForm[SortBy[newBB3, Length]]

```

